ACS OMEGA

http://pubs.acs.org/journal/acsodf

Perspective

Fomite Transmission, Physicochemical Origin of Virus−Surface Interactions, and Disinfection Strategies for Enveloped Viruses with Applications to SARS-CoV-2

Nicolas Castaño,[‡] Seth C. Cordts,[‡] Myra Kurosu Jalil,[‡] Kevin S. Zhang,[‡] Saisneha Koppaka, Alison D. Bick, Rajorshi Paul, and Sindy K. Y. Tang*

Cite This: *ACS Omega* 2021, 6, 6509−6527

Read Online

ACCESS | Metrics & More | Article Recommendations

ABSTRACT: Inanimate objects or surfaces contaminated with infectious agents, referred to as fomites, play an important role in the spread of viruses, including SARS-CoV-2, the virus responsible for the COVID-19 pandemic. The long persistence of viruses (hours to days) on surfaces calls for an urgent need for effective surface disinfection strategies to intercept virus transmission and the spread of diseases. Elucidating the physicochemical processes and surface science underlying the adsorption and transfer of virus between surfaces, as well as their inactivation, is important for understanding how diseases are transmitted and for developing effective intervention strategies. This review summarizes the current knowledge and underlying physicochemical processes of virus transmission, in particular via fomites, and common disinfection approaches. Gaps in knowledge and the areas in need of further research are also identified. The review focuses on SARS-CoV-2, but discussion of related viruses is included to provide a more comprehensive review given that much remains unknown about SARS-CoV-2. Our aim is that this review will provide a broad survey of the issues involved in fomite transmission and intervention to a wide range of readers to better enable them to take on the open research challenges.

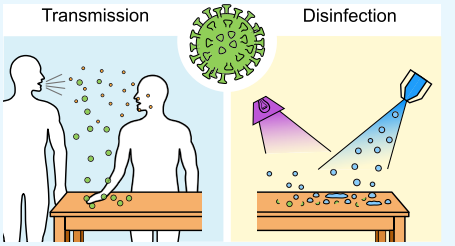

1. INTRODUCTION

As of 28 December 2020, the COVID-19 pandemic has infected >81 million and caused >1.7 million deaths worldwide,[1] significantly more than Middle East respiratory syndrome (MERS) and severe acute respiratory syndrome (SARS) combined.[2] In general, the primary routes of respiratory virus transmission are (1) direct contact between individuals, (2) indirect contact via fomites, which are inanimate objects that can become contaminated and transmit infectious agents, and (3) airborne transmission via droplets and aerosols.[3]

There is growing consensus that contaminated fomites play a critical role in the spread of viruses in a wide range of environments,[4−7] including hospitals, nursing homes, schools, offices, and restaurants.[4,8] Surface disinfection is one of the strategies used to intercept fomite-based disease transmission. Chemical disinfectants, such as bleach and ethanol, are commonly used to sanitize surfaces. For large-scale and/or outdoor surface disinfection, mass spray chemical disinfection is also currently used in various countries,[9−11] via robots, unmanned aerial vehicles, and other semi-autonomous or autonomous spray equipment. UV irradiation has also been applied to disinfect, for example, vehicles for public transportation.[12] While these disinfection strategies can have multiple potential benefits, the effectiveness of some methods, especially for the control of COVID-19, has not been fully examined.

The science of fomite transmission and interception is complex, and much active research is still ongoing for SARS-CoV-2. Understanding the basic principles underpinning the interactions between viruses and surfaces, as well as their inactivation, is important for a better understanding of how the disease is transmitted, how to intercept the transmission, and, eventually, how to devise guidelines to prevent the spread of the disease. The overall goal of this review is to provide a broad survey of the issues involved to provide readers who are nonspecialists with the background information needed to contribute to the research. Specifically, we (1) review the current knowledge and underlying physicochemical processes of virus transmission, in particular via fomites, and common disinfection strategies and (2) identify gaps in knowledge and areas in need of further research. Although the review focuses on SARS-CoV-2, the virus responsible for COVID-19, it

Received: December 30, 2020
Accepted: February 19, 2021
Published: March 5, 2021

https://doi.org/10.1021/acsomega.0c06335
ACS Omega 2021, 6, 6509−6527

Table 1. Surrogate Viruses for SARS-CoV-1/SARS-CoV-2

surrogate viruses	virus family	host cells	BSL	references
TGEV (transmissible gastroenteritis virus)	Coronaviridae	swine testicular cells (ST cells) porcine kidney cells (PK15 cells)	BSL 2	39−42
PEDV (porcine epidemic diarrhea virus)	Coronaviridae	African green monkey kidney cells (Vero 76 cells) porcine intestinal epithelial cell line (IPEC-J2 cells)	BSL 2	42, 43
MHV (mouse hepatitis virus)	Coronaviridae	mouse epithelial cell line (NCTC) mouse delayed brain tumor cell (DBT cells)	BSL 2	39−41, 44
CCV (canine coronavirus)	Coronaviridae	dog fibroblast cells (A-72 cells)	BSL 2	45, 46
Phi6	Cystoviridae	*Pseudomonas syringae*	BSL 1	47−50

includes discussions of related viruses because much about SARS-CoV-2 remains unknown. We hope that this review provides value by stimulating research efforts to further our understanding of the transmission of the disease, as well as by facilitating the development and implementation of effective disinfection strategies.

The remainder of this review is organized as follows. Section 2 provides a short summary of the structure of SARS-CoV-2 as it relates to its transmission via fomites and inactivation. Section 3 summarizes the different routes of virus transmission and how viral load is quantified. Section 4 focuses on virus transmission via fomites, starting with a brief discussion of the physicochemical origin of virus adsorption to and transfer between surfaces, followed by a summary of empirical findings of the transfer rate and persistence of viruses on different surfaces. Section 5 reviews the inactivation mechanisms of viruses and current and emerging strategies used to intercept fomite transmission.

2. SARS-COV-2 STRUCTURE, ENVELOPE PROPERTIES, AND SURROGATE VIRUSES

This section focuses on the properties of SARS-CoV-2 that are directly relevant to their transmission via fomites and disinfection strategies. The details of the virus' structure, as well as other coronaviruses, can be found in previous works.[13−15]

2.1. Basic Structure. SARS-CoV-2 is a betacoronavirus, which is a genus of enveloped viruses with a linear, positive-sense, single-stranded RNA genome that encodes for four main structural proteins: envelope (E), membrane (M), spike (S), and nucleocapsid (N).[13] SARS-CoV-2, similar to other enveloped viruses, is composed of two structures: (1) a lipid bilayer envelope that surrounds (2) a nucleocapsid, a protein capsid enclosing the genome strand.[16]

The E, M, and S proteins are embedded in the lipid bilayer envelope. This lipid bilayer is derived from the host cell and is formed during the budding of a nucleocapsid through a cell membrane.[14] The lipid bilayer is susceptible to chemical disruption, for example, by surfactants. Disruption of the lipid envelope can render the virus inactive.[17] In addition to the lipid layer, the M and E proteins could be targets for the inactivation or weakening of SARS-CoV-2 due to their critical roles in viral envelope assembly and replication. While enveloped viruses are more susceptible to inactivation than nonenveloped viruses, they possess the ability to adapt the envelope molecular profile to evade immune systems.[17,18]

Compared with SARS-CoV-1, SARS-CoV-2 has ∼10- to 20-fold higher affinity for angiotensin-converting enzyme 2 (ACE2) receptors found on heart, lung, kidney, and intestinal cells.[19,20] Increased ACE2 affinity implies that a small dose of virus could be sufficient to impart an infection.[21−24] A recent review summarized infective doses of SARS-CoV-2 in various animal models.[21] African green monkeys became infected with an aerosolized dose of SARS-CoV-2 as low as ∼1380 $TCID_{50}$ (50% tissue culture infective dose).[25] In humans, SARS-CoV-1, a similar strain as SARS-CoV-2, was postulated to have an infective dose of ∼13 $TCID_{50}$.[26] The low infective dose and high ACE2 affinity, along with the long persistence of SARS-CoV-2 on the skin and other surfaces (Section 4.2), could contribute to the spread of COVID-19 via fomites.[6,24,27]

2.2. Physicochemical Properties. The diameter of the ellipsoidal SARS-CoV-2 virion ranges from ∼65 to ∼97 nm (for the short and long axes of the envelope).[28] The isoelectric point (pI) of viruses is important in determining their adsorption characteristics (see Section 4.1). Based on the protein composition, the pI values of the M and N proteins of other coronaviruses have been computed theoretically to be ∼9.3−10.7.[29−31] The pI values of the M and N proteins on SARS-CoV-2 are likely to be within the same range. Although the overall isoelectric points of coronaviruses have not been reported, they are expected to be largely influenced by the isoelectric properties of M and N proteins[31,32] and can be further approximated by accounting for the dissociation constants of all amino acids of the virus.[33]

2.3. Surrogates. SARS-CoV-2 requires biosafety level (BSL) 3 facilities to handle.[34] To facilitate research on its infectivity, transmission, and disinfection, surrogates are often used. The first class of surrogates involves the use of natural viruses with low infectivity in humans. Table 1 shows these surrogate viruses, the host cells, and the BSL levels reported thus far. These surrogates are enveloped viruses with an RNA genetic material. They are used as surrogates because they are typically in the Coronaviridae family and have a similar structure to SARS-CoV-2 but are noninfective to humans, making them safer to study than SARS-CoV-2.

A second class of surrogates is pseudotyped viruses. They are derived from parent viruses such as the murine leukemia virus (MLV), human immunodeficiency virus (HIV), and herpes simplex virus (HSV). The genomes of the parents are modified for safer use in BSL 2 labs.[35] The synthesis of pseudotyped viruses is highly adaptable and allows for the incorporation of various kinds of envelope glycoproteins.[36,37] For example, SARS-CoV-2 S glycoprotein has been incorporated into a lentiviral pseudotyped virion system to determine the potential drug targets for the virus.[38]

A third class of surrogates involves artificial capsids that emulate the viral architecture. For example, peptide capsids have been constructed using capsid proteins to serve as nonpathogenic viral surrogates.[51] They have been used to study aspects of viral infectivity, applied as antimicrobial agents to disrupt bacterial lipid bilayer membranes, and programmed

https://doi.org/10.1021/acsomega.0c06335
ACS Omega 2021, 6, 6509−6527

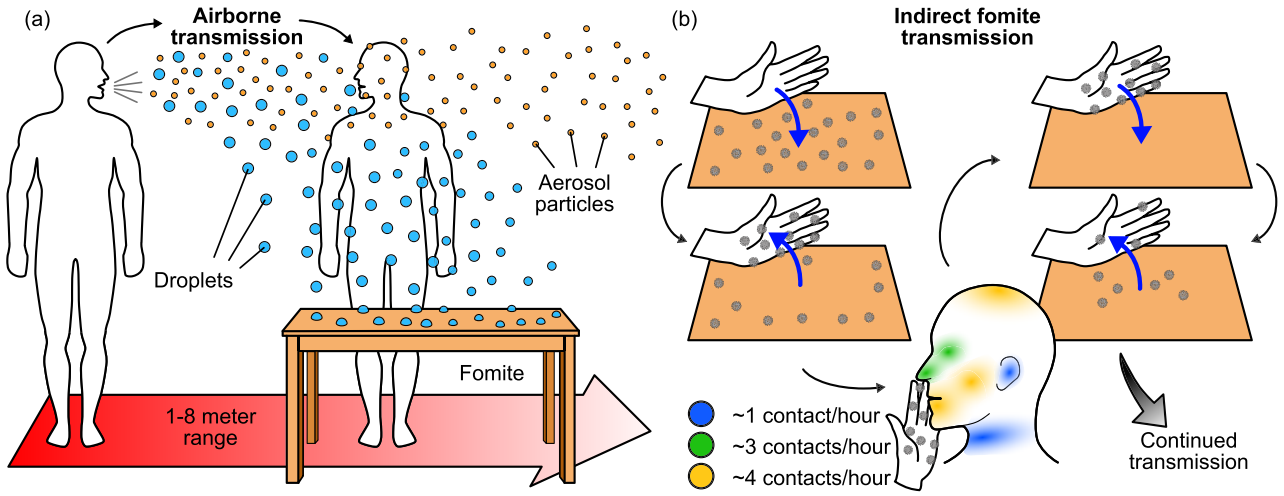

Figure 1. (a) Respiratory droplets and aerosol particles produced by an infected host during coughing/sneezing, talking, or exhaling can infect fomites or another individual directly. Droplets settle and adsorb onto fomites, while aerosol particles can remain suspended in air for minutes to hours.[55,61] (b) Indirect fomite-mediated transmission to a new human host occurs through contact with the fomite and subsequent contact with regions through which a virus can enter the body. Contact times can range from ∼1 to 50 s.[67] Virus particles can also be transferred to a surface via touch from contaminated skin (blue arrows).

to carry a specific genetic cargo and deliver it into the cytoplasm of human cells.

3. VIRUS TRANSMISSION: GENERAL ROUTES AND MEASUREMENTS OF VIRAL LOAD

3.1. Transmission Routes of Viruses. Understanding the transmission routes of viruses is crucial to the development of effective control measures. Three primary transmission routes have been found to contribute to the spread of respiratory viruses (e.g., SARS-CoV-1 and SARS-CoV-2, measles, human coronavirus (HCoV), rhinovirus, and influenza virus) (Figure 1a): (1) direct contact between individuals, (2) indirect contact via contaminated objects (fomites), and (3) airborne transmission via droplets and aerosols.[3,52]

Direct contact involves the transmission of the virus through physical contact between an infected host and a susceptible individual. Direct contact is a potent transmission route since the viral load can be large, and the virus spends a shorter amount of time outside of a host compared with other routes of transmission. Close-proximity airborne transmission can present as a form of direct transmission. For MERS, SARS-CoV-1, and SARS-CoV-2, direct contact and airborne transmission are considered to be major routes of viral spread.[53,54]

Indirect contact involves the transmission of the virus through a contaminated intermediate object, i.e., a fomite. Fomites can become contaminated either by the physical contact with another infected fomite or skin or by settling airborne particles. Fomite transmission can occur when an individual touches a contaminated fomite and then touches their facial membranes (Figure 1b). Numerous studies have implicated fomites as a significant virus transmission route in a range of environments.[4,8] At least one study implicated fomites as a likely mode of transmission in a cluster of COVID-19 cases in Wenzhou, China.[5] Although the transfer efficiency of SARS-CoV-2 from fomites to other fomites or skin is not well characterized, the transfer efficiency of a number of viruses has been investigated and will be detailed in Section 4.

Respiratory viruses can also become airborne and spread via particles generated by sneezing, coughing, talking, or exhaling. These airborne droplets and aerosols can cause infection through inhalation into the respiratory tract[55] or by settling onto fomites.[4] The particles generated can be classified into droplets or aerosols with a traditional cut-off diameter of 5−10 μm.[3,52,56,57] This cut-off is based on the tendency of the particle to remain suspended in air and the deposition pattern in the lungs. Due to their large size, droplets can fall within 1−2 m of the source within seconds (Figure 2).[55,58] However,

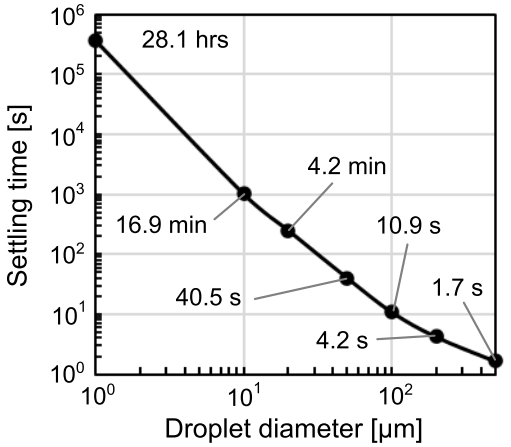

Figure 2. Droplet settling time from a height of 3 m was approximated based on its terminal velocity. In this approximation, settling timescales with the second power of droplet diameter and the air around the droplet is assumed to be stagnant. We generated this plot using published data.[73]

there is growing evidence that droplets can travel extended distances of up to 7−8 m under certain environmental conditions and contribute to airborne transmission.[59−61] For this reason, some studies have cautioned against the use of an oversimplified 5−10 μm cutoff to categorize airborne vs droplet transmission.[62,63] Indeed, recent studies indicated that a cut-off of 100 μm is more appropriate.[64,65]

Depending on the environmental conditions, aerosols can remain suspended in air for minutes to hours (Figure 2).[55,61]

https://doi.org/10.1021/acsomega.0c06335
ACS Omega 2021, 6, 6509−6527

Table 2. List of Important Viral and Fomite Properties that Impact the Adsorption, Transfer, and Persistence of Virus Particles on a Surface

property	impact	references
Surfaces		
surface charge	The net surface charge of an adsorbing surface, positive or negative, can either attract or repel a virus particle of an opposite or matching charge, respectively.	7, 92, 103
surface hydrophobic groups	Increased incidence of hydrophobic groups on the fomite surface increases the rates of virus adsorption by the hydrophobic effect.	94, 98, 100, 103−105
dielectric susceptibility	Materials with increased dielectric susceptibility result in increased rates of adsorption by van der Waals forces.	92, 93, 105, 107
porosity	Porous surfaces are less efficient than smooth surfaces in transferring virus particles, but they can be better for harboring viruses.	111, 125
resident microfauna	Microfauna biofilms can slow down virus inactivation, but their proteases and enzymes can reduce virus viability.	117−120
resident protein	A surface coating of albumin proteins increased virus persistence, but the effect of a more complex and physiologically relevant protein coating is less understood.	121−123
presence of metal ions	Intrinsic antimicrobial properties of some metals (e.g., copper) inactivate viruses in <30 min through various modes of action involving interactions of proteins with metal ions (see Section 5.3.1).	126−131
Virus particles		
overall isoelectric point (pI) of viral membrane or capsid	Individual amino acids and polypeptide chains determine the effective charge on viruses that dictate long-range electrostatic interactions.	29−32, 92, 99
surface hydrophobic groups	Increased incidence of hydrophobic groups on the virus surface increases the rates of adsorption by the hydrophobic effect.	94, 98, 100, 103−105
presence of envelope	Enveloped viruses are typically more susceptible to inactivation.	39, 111, 122, 124

Such prolonged suspension could increase the distance the virus travels from the source and the number of individuals and fomites exposed to the virus. Airborne droplets and aerosols can also deposit onto and contaminate fomites. A study on SARS-CoV-2-infected patients in isolation rooms showed contamination of high-contact surfaces such as doorknobs and bedrails, as well as air outlet fans, which indicated virus transfer from aerosols to a surface.[66]

While the transmission routes discussed above are generally accepted as the primary transmission routes of respiratory viruses, sewage, dust-borne,[68] and "aerosolized fomite" transmission[69] have also been implicated as possible routes. Live SARS-CoV-2 has been detected in stool samples,[70] and both SARS-CoV-1 RNA and SARS-CoV-2 RNA have been detected in wastewater,[71,72] suggesting the possibility of transmission via the fecal-oral route or via aerosolization of sewage caused by flushing.

Even though these routes have been identified, the relative importance of each transmission route in the spread of SARS-CoV-2 and most respiratory viruses remains an open question. Furthermore, there is often a confounding effect between transmission routes. For example, persons in sufficiently close proximity for droplet-based transmission are likely exposed to a great load of virus-laden aerosols simultaneously.[74] In a model of influenza infection assessing the relative contributions of each transmission route to infection risk within a household, fomite transmission was estimated as a major, if not the dominant, transmission route.[75] Although the importance of each transmission route remains poorly understood, there is a growing consensus that contaminated fomites play a critical role in the spread of viruses.[4]

3.2. Measurement of Virus Infectivity. In this section, we summarize the current collection and analysis methods of viruses from fomites. A discussion of the methods for collecting aerosolized viruses is outside the scope of this review, but they are covered in previous studies.[76−79]

3.2.1. Surface Sample Collection. In a recent study monitoring the presence of SARS-CoV-2 RNA on high-touch surfaces in the community,[80] a swab collection method was used where polypropylene swabs were saturated in phosphate-buffered saline (PBS). The surfaces were swabbed entirely, while the swab was rotated throughout the process. In this study, the efficacy of the swab collection method was tested separately with bovine coronavirus (BCoV). Using metal and plastic surfaces to measure the recovery efficiencies, 16 and 38% of initial BCoV RNA were recovered, respectively. In a different study looking at nonenveloped viruses, the most effective method for recovering MS2 bacteriophages from nonporous fomites used polyester-tipped swabs prewetted in either one-quarter-strength Ringer's solution or saline solution.[81] This method recovered a median fraction of 40% for infective MS2 and 7% for MS2 RNA from stainless steel and PVC surfaces. Using 0.05 M glycine buffer, another study showed comparable recovery efficiency between aspiration and swabbing methods. A combination of aspiration and scraping yielded ∼71% virus recovery.[82] Despite these past studies, more research is needed to examine the collection efficiency of enveloped viruses, including SARS-CoV-2, from surfaces, as well as to standardize the methods used. Without this knowledge, the quantification of viral load on fomites remains unreliable.

3.2.2. Quantification of Infectious Virus and Nucleic Acid Concentration. The two prevailing methods for detecting viral nucleic acids and viable virus particles are reverse transcriptase polymer chain reactions (RT-PCR) for RNA (or PCR for DNA) and cell culture assays. RT-PCR assays are well characterized, are straightforward to perform, and do not require cell culture. Their limitation lies in the inability to determine virus infectivity.[83] For cell culture assays, recent publications have used Vero E6 cells to quantify the presence of infective SARS-CoV-1 and SARS-CoV-2.[84−88] While cell culture assays are the most popular method for determining infectivity, they have several limitations, including the long duration of the assay (possibly exceeding a week) due to the time required for observable cytopathic effects.[83,89]

Most current methods take a few hours to measure virus RNA/DNA concentration and days to measure virus infectivity. Additionally, most methods require instrumentation and/or cell culture that may be inaccessible and impractical for virus tracking and regular verification of successful surface

https://doi.org/10.1021/acsomega.0c06335
ACS Omega 2021, 6, 6509−6527

disinfection. Rapid tests for virus genetic material and infective virus could be useful for community monitoring in highly trafficked areas such as public transportation sites, restaurants, and hospitals and could be used to signal potential outbreaks before the detection in patients.[80] Rapid testing is also important for the verification of successful disinfection of surfaces between human uses (e.g., between rides in taxis or uses of public restrooms). Therefore, there is an unmet need for the rapid detection (less than 1-2 hours) of viable infective virus not only from patient samples but also from aerosols, droplets, and fomites to both improve the basic understanding of the infection risk via these transmission routes and to reduce the detection time so that measures can be taken to prevent outbreaks.

4. VIRUS TRANSMISSION VIA FOMITES

The ability of a virus to transfer between and persist on different surfaces, including the human skin, plays a crucial role in the overall infectivity of a virus by means of fomite transmission. Understanding the adsorption and transfer characteristics between the skin and fomites is critical for modeling the spread of viruses[8,90] and can provide insight into potential targets to prevent adsorption of viruses onto inanimate and biological surfaces (e.g., skin and mucosal lining). Furthermore, understanding virus persistence on different surfaces under different environmental factors can inform decision-making for disinfection protocols. This section reviews the factors affecting virus adsorption, transfer, and persistence on different surfaces and then discusses surfaces that are at high risk of contamination.

4.1. Physicochemical Origin of Virus Adsorption and Transfer. The adsorption of viruses on fomites and their subsequent transfer to other surfaces is a multifactor problem that depends on the properties of the virus, the fomite, and the environment. A better understanding of the physicochemical processes involved could lead to more effective strategies to intercept fomite transmission.[7] Thus, this subsection contains significantly more technical detail than other sections because we believe that a better understanding of the fundamental processes could facilitate the prediction and modeling of high-risk surfaces, as well as the identification of effective and novel disinfection strategies that may modify the virus−surface interaction to prevent their adsorption. Table 2 summarizes important viral and fomite properties that impact the adsorption, transfer, and persistence of virus particles on a surface.

The physical description of virus adsorption borrows from formulations of colloid adsorption, treating virus particles as soft colloidal spheres and using Gibbs free energy to model the interactions between virus particles and the adsorbing surface. Like colloid adsorption on surfaces, virus adsorption onto fomites is primarily driven by electrostatic, hydrophobic, and van der Waals interactions (Figure 3). The relative contribution of these interactions is modulated by environmental pH and ionic strength.[4,7,90,91]

Classical models of virus adsorption adopt the Derjaguin−Landau−Verwey−Overbeek (DLVO) theory for colloid adsorption on surfaces. This theory accounts for electrostatic and van der Waals interactions between viruses and surfaces.[92−94] However, the extended-DLVO (XDLVO) model, which considers hydrophobic interactions, was found to agree more with experimental observations of virus

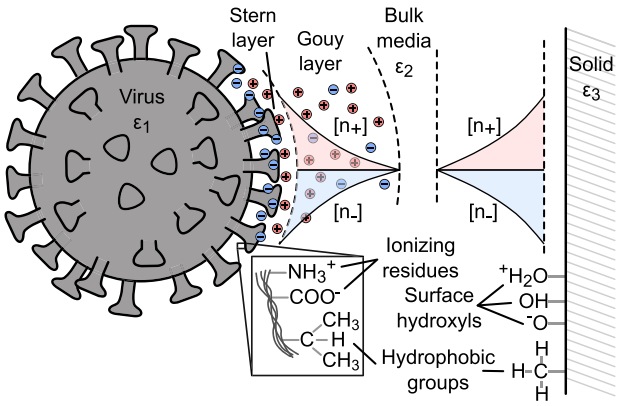

Figure 3. Diagram summarizing components contributing to XDLVO-based interactions between a virus and a surface. Ionizing residues on viral amino acids interact with surface hydroxyls groups on an adsorbing surface. The Gouy layer forms from a local imbalance in charge concentration. These long-range electrostatic forces are attractive or repulsive based on the charges on the virus and the surface. Apolar hydrophobic groups on the virus and surface exhibit shorter-range interactions. The complex dielectric susceptibility (ε) mismatch of the virus, media, and solid surface drives van der Waals interactions.[92]

adsorption.[95−97] XDLVO is expressed in terms of Gibbs free energy of interaction, as shown in eq 1 below

$$\Delta G_{total} = \Delta G_{dl} + \Delta G_{vdW} + \Delta G_{hyd} - T\Delta S_0 \quad (1)$$

where electrostatic or double-layer (dl), hydrophobic (hyd), and van der Waals (vdW) contributions are summed. Entropy changes (ΔS_0) are usually ignored. A negative ΔG_{total} favors adsorption.[93,94] Detailed formulations for each component of the total free energy for a spherical virus particle adsorbing onto a flat plate can be found in a prior work.[96]

Electrostatic forces drive long-range adsorption dynamics dictated by the radius of the virus' electrical double layer (Debye length) and the charge of the adsorbing surface.[92,98] All viruses, including SARS-CoV-2, express unique protein markers on their surfaces. These markers consist of weakly acidic or basic polypeptides and amino acid-ionizing residues that give viruses their characteristic isoelectric point (pI) values (also see Section 2.2).[7,92,99] The net charge of a virus is thus determined by its pI and the pH of its environment,[92] e.g., environmental pH below the pI of a virus particle results in an overall positive charge on the virion. The net charge on a virus causes the formation of an electrical double layer that extends from the Stern layer, the first layer of immobile charges attached to the surface of the virus particles, and across the Gouy diffuse layer, the region of charge imbalance that results in an electrical potential.[100−102] In addition to pH, the ionic strength of the surrounding medium is another important parameter that affects electrostatic interaction. At high ionic concentrations (e.g., >100 mM $NaNO_3$),[98] electrostatic screening stunts the zeta potential at the charge slipping plane and weakens the effects of surface charge for both attractive and repulsive interactions.

The hydrophobic effect contributes significantly to adsorption, especially when electrostatic interactions are absent.[98,100] Hydrophobic interactions lead to an attractive force between a virus particle and an adsorbing surface due to an electron-donor and electron-acceptor (i.e., Lewis acid−base) interfacial interaction. The hydrophobic effect is a shorter-range effect

https://doi.org/10.1021/acsomega.0c06335
ACS Omega 2021, 6, 6509−6527

Table 3. Summary of the Persistence of Human Coronaviruses along with Porcine and Murine Coronaviruses, TGEV and MHV, Respectively, which Are Commonly Used as Surrogates for Human Coronavirus[a]

virus	type/strain	quantification method	inoculum titer	surface type	relative humidity	temperature	viability period	ref
SARS-CoV	type 2	Vero E6 cell plaque assay	5 μL of 10^5 $TCID_{50}$/mL in DMEM	stainless steel	45−55%	25 °C	<84 h	150
				borosilicate glass			<86 h	
				polystyrene			<58 h	
				skin			<9 h	
			5 μL of 10^5 $TCID_{50}$/mL in mucus	stainless steel			<65 h	
				borosilicate glass			<61 h	
				polystyrene			<36 h	
				skin			<11 h	
		Vero E6 cell plaque assay	50 μL of 10^6 $TCID_{50}$/mL	aluminum	45−55%	19−21 °C	≤2 h	121
				aluminum with BSA			>96 h	
				glass			≤24 h	
				glass with BSA			>96 h	
				polystyrene plastic			>96 h	
				polystyrene plastic with BSA			>96 h	
		Vero E6 cell plaque assay and RT-PCR	5 μL of $10^{7.8}$ $TCID_{50}$/mL	cloth	65%	22 °C	≤2 days	84
				steel			≤7 days	
				glass			≤4 days	
				plastic			≤7 days	
	type 2	Vero E6 cell plaque assay and RT-PCR	5 μL of $10^{7.8}$ $TCID_{50}$/mL	wood	65%	22 °C	≤2 days	84
				bank note			≤4 days	
				paper, tissue paper			≤3 h	
				surgical mask			≤7 days	
	type 2/nCoV-WA1−202	Vero E6 cell plaque assay	50 μL of 10^5 $TCID_{50}$/mL	steel	40%	21−23 °C	≤72 h	88
				copper			≤4 h	
				plastic			≤72 h	
				cardboard			≤24 h	
	type 1/Tor2	Vero E6 cell plaque assay	50 μL of 10^5 $TCID_{50}$/mL	steel	40%	21−23 °C	≤72 h	88
				copper			≤8 h	
				plastic			≤48 h	
				cardboard			≤8 h	
MERS-CoV	isolate HCoV-EMC/2012	Vero E6 cell plaque assay	droplets, 5 μL of 10^6 $TCID_{50}$/mL	steel, plastic	40%	20 °C	≤48 h	151
					80%	30 °C	≤8 h	
					30%	30 °C	≤24 h	
HCoV	229E	L132 cell plaque assay	10 μL of 5.5 × 10^5 $TCID_{50}$/mL	aluminum, sterile sponge, latex glove	55−75%	22 °C	≤3 h	152
		MRC-5 cell plaque assay	10 μL of 10^3 PFU/cm^2	glass, PVC, Teflon, steel	30−40%	21 °C	≤5 days	153
				rubber silicon			≤3 days	
				copper nickel (>90% copper)			<30 min	
	OC43	HRT-18 cell plaque assay	10 μL of 5.5 × 10^5 $TCID_{50}$/mL	aluminum, sterile sponge, latex glove	55−75%	22 °C	<1 h	152
TGEV	not specified	swine testicular cell plaque assay	10 μL of 10^4−10^5 MPN/cm^2 (MPN is the most probable number of virus particles)	steel	20−80%	4 °C	>28 days	40
					20−80%	20 °C	3−28 days	
					20−80%	40 °C	4−96 h	
MHV	not specified	delayed brain tumor cell plaque assay	10 μL of 10^4−10^5 MPN/cm^2	steel	20−80%	4 °C	>28 days	40

[a]High levels of discrepancies in viability between similar virus−surface combinations could be attributed to experimental differences in environmental conditions and inoculum titer. The viability periods reported could also be underestimated since the viral counts may be underestimated due to sampling inefficiencies and detection limits of the plaque or $TCID_{50}$ assay.

than electrostatic interactions.[98,100] Under hydrophobic interactions, there is a tendency of apolar species, such as molecular chains or particles, to aggregate,[94] thereby providing an energetically favorable mechanism of adsorption due to the minimization of interfacial area between the virus and the adsorbing material.[103] In the absence of electrostatic interactions, hydrophobic effects dominate because they are apolar in nature. The energy of hydrophobic interactions largely depends on the prevalence of hydrophobic groups on a virus particle's surface. Greater virus hydrophobicity has been shown to correlate with higher rates of adsorption regardless of ionic strength.[98,104,105] The presence of chaotropic (e.g., SCN^- and Cl_3CCOO^-) or antichaotropic (e.g., NO_3^-, SO_4^{2-}, and F^-) agents can respectively promote or hinder hydrophobic adsorption.[92]

https://doi.org/10.1021/acsomega.0c06335
ACS Omega 2021, 6, 6509−6527

Van der Waals forces are of secondary importance.[7] Their relative contribution, as with electrostatic and hydrophobic interactions, is a function of virus and environmental properties. For example, van der Waals forces may play a significant role in the adsorption of viruses that carry a neutral charge in their environment.[106] Furthermore, materials known to generate large van der Waals potentials are also more likely to adsorb viruses.[92] The contribution of van der Waals forces to adsorption can be quantified by Lifshitz theory, which predicts that materials with higher dielectric susceptibility produce higher van der Waals potentials. By this reasoning, metals have better adsorbing effectiveness than most organic substances. In general, the effectiveness of materials to adsorb viruses follows metals > sulfides > transition metal oxides > SiO_2 > organics. The Lifshitz theory suggests that high ionic strength or a fluid pH equal to virus pI is necessary for adsorption to most organics. Under these conditions, the Debye length is shortened, and viruses are able to get sufficiently near to organic surfaces to adsorb by van der Waals interactions.[92,93,107]

There exist some gaps in the comprehensive understanding of the physicochemical mechanisms in virus adsorption onto fomites. While XDLVO theory can begin to explain the ready adsorption of many virus strains, including SARS-CoV-2, to a variety of nonporous surfaces (e.g., steel, glass, and plastic),[4,27,84,88,108] the observed virus adsorption onto porous fomite surfaces (e.g., cardboard and cloth) is not well described by XDLVO. Some studies have indicated the need to account for steric effects and surface roughness.[103,105] Other studies have emphasized the pitfalls of modeling viruses as soft colloids with homogeneous charge distributions. Unlike a soft colloid or even a virus-like particle (VLP) engineered with viral structural proteins, the pI of true viruses depends on the complex physicochemical structure of the outer surface and the genetic material packed within the capsid.[98,106,109,110]

Although the state of understanding in physicochemical mechanisms of virus adsorption in aqueous environments is fairly advanced, there is still a significant room for research in elucidating the mechanisms of dry contact transfer. For example, while a number of studies have quantified the rates of transfer between dry surfaces, including the skin (also see Section 4.2), the precise physicochemical basis for virus transfer in dry conditions has not been addressed. The tendency of a virus to transfer between fomites is likely determined by differences in adsorption energies between the two surfaces. In the case of porous materials, lower rates of transfer are likely due to viruses entrapped in their matrix due to increased surface area for attachment.[111,112]

4.2. Transfer Efficiency and Persistence of Coronaviruses and Surrogates on Different Surfaces. Although extensive studies have examined the transfer efficiency of viruses, few have focused on coronaviruses. Nevertheless, these studies have provided useful insights. In one study, an overall mean transfer efficiency of 23 ± 22% was found between fingerpads (either washed or unwashed prior to inoculation with a virus) and glass for three types of nonenveloped bacteriophages (MS2, φX174, and fr). The efficiency was calculated by measuring the viral PFU of the surface before and after contact. In this study, prior handwashing was found to reduce the transfer efficiencies only slightly. The reduction due to washing was greater in fingerpad-to-glass transmission than glass-to-fingerpad transmission. This result is likely because of changes in the skin moisture or pH due to handwashing before inoculation with a virus.[113] A similar transfer efficiency was found for MS2 from fingertips to glass and to acrylic (~20%), but this value increased to 79.5% in humid conditions.[112] Transfer efficiency of PSD-1 phages from hand to mouth was found to be 33.9%, representing a skin-to-skin pathway.[114] The enveloped bacteriophage Phi6 was shown to adsorb from skin to liquid with similar efficiency as nonenveloped MS2 and Qβ.[50]

Despite the lack of research on skin-to-surface transfer efficiency for coronaviruses, the persistence of coronaviruses on surfaces has been extensively quantified. Studies have shown that viruses adsorbed on surfaces can maintain high rates of survival and infection potential. Exactly how long viruses retain their viability on a surface is highly variable and dependent on (1) surface porosity, (2) environmental factors, and (3) virus envelope characteristics (also see Table 2).[109,128]

First, nonporous surfaces are more prone than porous surfaces to receive and transfer viruses, and they typically preserve virus viability longer than porous surfaces because they do not draw moisture away from adsorbed viruses.[111] However, if a porous material is inoculated, then it is capable of harboring most strains of viruses (especially at low temperatures, e.g., 4 °C), and the material can remain as a source of contagion despite the lower rates of transfer to the skin.[109] Of note is SARS-CoV-2's demonstrated ability to contaminate a wide range of nonporous and porous fomites. Table 3 shows the persistence of SARS-CoV-2 and other coronaviruses on various surfaces. On the skin, SARS-CoV-2 demonstrated a significantly longer persistence than influenza A virus (~9−11 h vs ~1.75 h).[129] No work, to our knowledge, has explicitly investigated the physicochemical reasons behind the ability of some surfaces to support longer virus persistence. However, because viruses can be inactivated by desiccation,[35] improved persistence can be related to the ability of a surface to maintain a moist microenvironment.

Second, environmental variables such as temperature, humidity, resident microfauna, and proteins can influence virus adsorption and viability. In general, increased temperature and moderate humidity levels have adverse effects on the persistence and viability of coronaviruses and other viruses.[43] One recent quantification of SARS-CoV-2 persistence on smooth surfaces under different temperatures and humidities showed a decrease in virus persistence with increasing relative humidity (20 to 80%) at 24 and 35 °C.[115] In a study on the viability of dried SARS-CoV-1 on smooth plastic surfaces, the virus was found to be viable for over 5 days at 22−25 °C with 40−50% relative humidity (RH). However, virus viability decreased significantly (>3 $\log_{10}$ reduction) at 38 °C with >95% RH.[116] In another study using Phi6 as a surrogate, the virus survived best at high (>85%) and low (<60%) RHs. They also found that RH is a more significant factor in virus survivability than absolute humidity (AH).[47] In addition to temperature and humidity, the presence of other microbes can also influence the survival of viruses.[117] Although the presence of microbes and their biofilms can reduce the rate of desiccation of the viral particles,[111,118,119] thereby enhancing virus persistence, microbial proteases and fungal enzymes can be harmful to virus viability.[117,120] Coating aluminum and glass with BSA proteins, at a concentration representative of proteins in respiratory fluids, has also been shown to enhance the viability of SARS-CoV-2, likely due to increased protection from drying.[121−123]

https://doi.org/10.1021/acsomega.0c06335
ACS Omega 2021, 6, 6509−6527

Third, viral persistence on fomites also depends on the type and the strain of the virus. In general, enveloped viruses have shorter persistence on fomites than nonenveloped enteric viruses (e.g., adenovirus and rotavirus).[4] The presence of a lipid membrane in enveloped viruses makes them more susceptible to inactivation than nonenveloped viruses. The disintegration of the lipid envelope (e.g., by common disinfectants; see details in Section 5) causes the loss of the viral envelope proteins involved in virus adsorption and cell penetration, rendering them inactive.[17] Additionally, enveloped viruses are more susceptible to desiccation than their nonenveloped counterparts because of their lipid membrane envelopes.[111,122] Loss of water molecules in lipid membrane envelopes can cause the cross-linking of functional groups found on the membrane, peroxide formation, Maillard reactions, and phase changes.[40,124] These characteristics make it more difficult for enveloped viruses to spread and persist on surfaces over long periods of time compared with nonenveloped viruses.[111]

4.3. Surfaces at High Risk of Virus Contamination. In principle, all surfaces or objects can be considered fomites given that they can be at risk of contamination and transmission of viruses.[4,8] In practice, knowing which objects are at high risk of contamination would better guide disinfection strategies. For a given object, the risk of contamination can depend on the interaction between the virus and the material, the frequency at which the object is contacted, the object's distance from an infected individual, and the environmental conditions.

First, the combination of virus composition and surface properties can influence the likelihood of contamination (see details in Section 4.1). Second, objects that are frequently handled or are in high contact with individuals are at higher risk of contamination. In a hospital setting, contamination has been detected on numerous high-contact surfaces, including door handles, bed rails, tables, call/control panels, other near-patient surfaces, office equipment, and even sterile packaging.[126,132] A study of the isolation rooms of SARS-CoV-2-infected patients in Singapore showed contamination of a similar list of high-contact surfaces.[66] While the floor of the isolation room and the shoes worn by individuals entering and exiting the room tested positive for SARS-CoV-2, the floor immediately outside tested negative, suggesting contamination by footwear is low. A recent environmental surveillance study was able to detect trace levels of SARS-CoV-2 RNA on high-touch public surfaces and locations, where trash cans had the highest frequency of SARS-CoV-2-positive samples, followed by the door handle of liquor stores.[80]

Third, an object's proximity to an infected individual affects its risk of contamination. An object can be contaminated from a distance due to deposition of droplets or aerosols on its surface. Although the risk of contamination by droplets or aerosols decreases when the object is further away from infected individuals, viral shedding by coughing, sneezing, or exhaling can potentially deposit droplets and aerosols onto fomites as far as 8 m away, subjecting objects within that range to contamination.[59,60] In a study in Singapore, all air samples taken from the isolation room tested negative, while the air outlet fans tested positive, suggesting that SARS-CoV-2 is not detectably aerosolized in these conditions but is still able to transfer from air to a potential fomite that is actively moving through the air, as was the fan circulating air out of the room.[66] A study in Wuhan hospitals found that the highest concentrations of SARS-CoV-2 in the air were, surprisingly, not in patient rooms but in toilet facilities.[133] Even aerosol generation from personal protective equipment (PPE) removal can create fomites. Doffing PPE has the potential to aerosolize the virus and transfer it to other PPE in changing rooms.[133]

Fourth, environmental conditions can affect an object's risk of contamination. Air currents could potentially determine the flight path of droplets and aerosols,[59] as proposed in a case study of a Guangzhou restaurant where the SARS-CoV-2 infection pattern aligned with the air conditioning currents.[134] The amount of foot traffic and the degree of connectivity between rooms could also affect where high SARS-CoV-2 concentrations may be found.[135] We note that a limitation to many of these studies is the use of RT-PCR to identify viral RNA. The presence of viral RNA is not indicative of viability, and viral culture is needed to determine infective viruses.[81]

The above factors can be used to identify and predict surfaces at high risk of contamination. To further quantify the role of these surfaces as fomites, surface viral concentrations need to be measured, and contact frequencies can be derived from observational studies.[80,126,136,137] Such quantifications can be used as input parameters in modeling infection risk and designing optimal disinfection strategies. Kraay et al. introduced a model to predict the fomite-mediated reproductive number, or outbreak potential, of influenza, rhinovirus, and norovirus given the parameters specific to the virus (e.g., inactivation rate and transfer efficiency), the environment (e.g., touch rate), and the cleaning rate.[90] Another study incorporated the contribution of droplet- and aerosol-mediated transmission.[137] Readers are referred to a recent review of modeling approaches in virus transmission that encapsulates models from aerosol dispersion to biological uptake of viruses in the body.[52] Further quantification of model inputs that reflect virus viability and transferability could serve to refine and validate current or future model parameters for SARS-CoV-2 transmission models.

5. STRATEGIES TO INTERCEPT THE FOMITE TRANSMISSION ROUTE

Current strategies to intercept fomite transmission of viruses revolve around inactivating the virus, improving personal hygiene, or using PPE. This section first discusses various mechanisms of virus inactivation on surfaces and hands and then focuses on strategies that have been shown to inactivate SARS-CoV-2 and other enveloped viruses. PPE is not discussed because it has been discussed in depth elsewhere.[138−147]

5.1. Reactivity of Viral Structures with Disinfecting Agents. In order for a virus to be infective, it must fuse with a host cell, insert its genome into the cell, and replicate.[148] These processes require an enveloped virus to have an intact envelope and nucleocapsid. To inactivate a virus, at least one of these components needs to be disrupted.[83]

It is important to understand the mechanisms of virus inactivation based on virus composition, structure, and function to (1) understand the efficacy of disinfectants on viruses, (2) predict the response of a new strain of virus to a disinfectant, (3) identify common sites on proteins, envelopes, or genomes that are vulnerable to disinfectant treatment that are shared by many viruses, and (4) enhance the design of antiviral agents and therapies that target specific viral components.[149]

https://doi.org/10.1021/acsomega.0c06335
ACS Omega 2021, 6, 6509−6527

Table 4. List of Disinfectants and Their Reactivity with Monomers of Virus Structures: Nucleotides and Amino Acids[149]

		disinfectant type		
	nucleotides and amino acids	UVC (254 nm)	free chlorine	ozone
reactivity with nucleotides; second-order rate constant, k [M^{-1} s^{-1}], reported for chlorine and ozone; molar attenuation coefficient, ε [M^{-1} cm^{-1}], reported for UVC	adenine	1.2×10^4	6.4	200
	cytosine	3.5×10^3	66	1.4×10^3
	guanine	1.0×10^4	2.1×10^4	5.0×10^4
	uracil	7.8×10^3	5.5×10^3	650
	thymine	6.3×10^3	4.3×10^3	1.6×10^4
reactivity with amino acids; second-order rate constant, k [M^{-1} s^{-1}], reported for chlorine and ozone; molar attenuation coefficient, ε [M^{-1} cm^{-1}], reported for UVC	cysteine		3.0×10^7	$\sim 1 \times 10^9$
	histidine		1.0×10^5	$\sim 4 \times 10^5$
	lysine		5.0×10^3	
	methionine		3.8×10^7	$\sim 6 \times 10^6$
	phenylalanine	140		
	tryptophan	2.8×10^3	1.1×10^4	~ 1 x 10^7
	tyrosine	340	44	$\sim 4 \times 10^6$
	backbone N		≤ 10	
	α-amino		1.0×10^5	

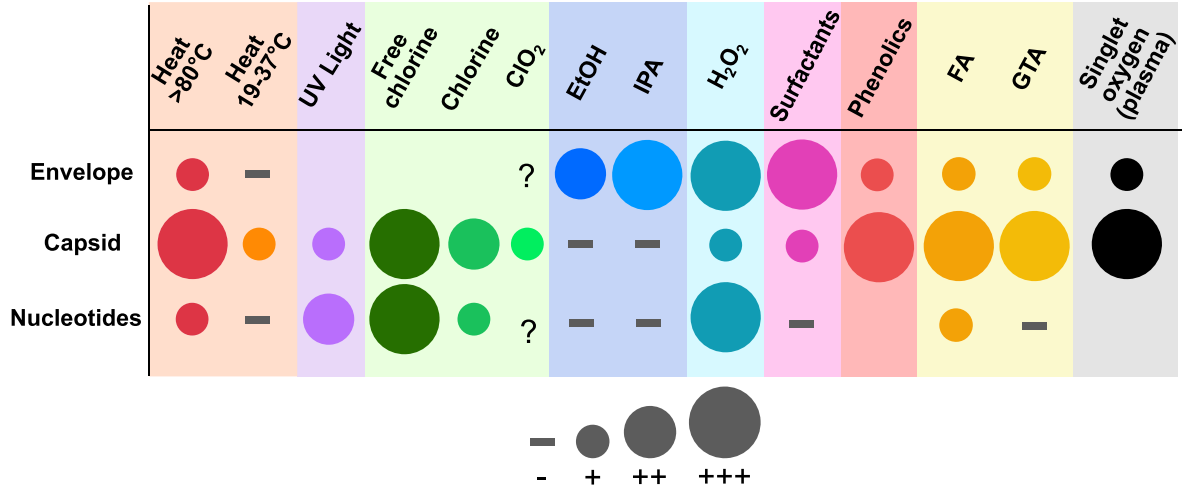

Figure 4. Viral structures targeted by different disinfectants. Symbol abbreviations: +, light damage; ++, moderate damage; +++, severe damage; −, no damage; ?, uncertain/debated. Chemical abbreviations: ClO_2, chlorine dioxide; EtOH, ethanol; IPA, isopropanol; H_2O_2, hydrogen peroxide; FA, formaldehyde; GTA, glutaraldehyde.[83] References: heat,[148,155,177] UV light,[148,177−180] chlorines,[148,181] EtOH and IPA, H_2O_2,[157] surfactants,[17] phenolics,[157] FA and GTA,[182,183] and singlet oxygen.[148,179,184]

One method of predicting virus inactivation mechanisms is a composition-based method. It takes into account the reaction rate constants between disinfectants and specific nucleotides and amino acids found in viral structures (e.g., proteins, nucleic acids, and envelope lipids) (Table 4). The relative contribution of a viral structure to inactivation can be predicted by summing the relative abundance of each nucleotide or amino acid multiplied by the respective rate constants for a given disinfectant.[33,149] A limitation of the composition-based method is that it does not account for the complex interactions between adjacent monomers.[149] To our knowledge, no model exists that accounts for the viral structure as well as composition.

5.2. Surface Disinfection Strategies. Current disinfection strategies and their effectiveness for SARS-CoV-2 and related viruses are discussed in the following sections and summarized in Figure 4.

5.2.1. Chemical Disinfectants. A wide variety of chemical disinfectants are currently available to combat the spread of SARS-CoV-2 (Table 5).[27,154] The effectiveness varies depending on the virus inactivation mechanism. In general, there are three modes of inactivation by disinfectants: (1) disruption of the lipid layer of the envelope (e.g., ethanol and detergents),[83,155] (2) modification of important protein sites on the envelope or capsid (e.g., chlorine and glutaraldehyde),[83,148,149,156,157] and (3) reaction with the nucleotides and amino acids in the genetic material, leading to the degradation of the nucleic acids (e.g., chlorine).[83,148]

Chemical disinfectants are typically evaluated with suspension and carrier tests. Suspension tests combine a known titer of a virus in solution with a disinfectant and evaluate virus titer after a period of time that is given in the disinfectant manufacturer's directions for use.[158] However, suspension tests are considered less challenging for the disinfectant under scrutiny[159] and may not reflect the practical usage of disinfectants to clean contaminated surfaces. Quantitative carrier tests are performed by allowing an aliquot of virus solution to dry on a surface before applying the disinfectant. This test is conducted under conditions that are more relevant to practical use of disinfectants, and it is, therefore, a more appropriate measure of disinfectant effectiveness.[159]

https://doi.org/10.1021/acsomega.0c06335
ACS Omega 2021, 6, 6509−6527

Table 5. Advantages, Disadvantages, and Hazards of Disinfection Techniques that Have Been Shown to Inactivate SARS-CoV-2 and Similar Coronaviruses[a]

disinfecting agent	hazards	advantages	disadvantages
UVC light (245 nm)	adverse health effects from irradiation[171]	Inactivates SARS-CoV-2 within 6 min.[172] UV light may be applicable to surfaces sensitive to heat or chemicals.	UV lamp irradiation is less efficient at low temperatures (e.g., <20 °C) and high humidity (e.g., >60% RH) and is not suitable for all environments.[196] Incompatible with photosensitive materials.
1, 2, and 10% sodium hypochlorite (bleach)	[3, 0, 1]* 12.5 wt %[197]	Inactivates SARS-CoV-2 within 5 min.[84,160] Sodium hypochlorite (0.21%) inactivates MHV in 30 s in carrier test.[198] Inexpensive and readily available.	
70% ethanol	[2, 3, 0]* 100 wt %[199]	Inactivates SARS-CoV-2 within 5 min.[84] Ethanol (>80%) inactivates SARS-CoV-1 within 30 s.[163] Leaves no chemical residue. Inactivates HCoV-229E, MHV, and TGEV within 1 min in carrier test.[41,166] Inexpensive and readily available.	
7.5% povidone-iodine	[2, 1, 0]* 100 wt %[200]	Inactivates SARS-CoV-2 within 5 min.[84] Inactivates MERS-CoV in 15 s.[164] Inexpensive and readily available.	
0.05% chloroxylenol	[1, 1, 0]* 3 wt %[201]	Inactivates SARS-CoV-2 within 5 min.[84] Inexpensive and readily available.	Inactivation effectiveness depends on the virus structure.[83] Chemical disinfectants may be incompatible with some metals and may stain substrates.
0.05% chlorhexidine	[1, 0, 0]* 2 wt %[202]	Inactivates SARS-CoV-2 within 5 min.[84] Inexpensive and readily available.	
0.1 and 0.19% benzalkonium chloride	[3, 1, 0]* 50 wt %[203]	0.19% benzalkonium chloride inactivates SARS-CoV-2 within 2 min in carrier test.[165] Inexpensive and readily available.	
50% ethanol and 0.083% alkyl (50% C14, 40% C12, and 10% C16) dimethyl benzyl ammonium saccharinate	[1, 3, 0]*[204]	Inactivates SARS-CoV-2 within 2 min in carrier test.[165] Inexpensive and readily available.	
heat (>70 °C)	igniting combustibles	Sources of heat (ovens and autoclaves) readily available.	Not applicable to heat-sensitive surfaces. Takes ∼1 h or more to inactivate SARS-CoV-2 on surfaces.[147]
cold atmospheric plasma	(active area of research)	Inactivates SARS-CoV-2 within 3 min.[205] Safer alternative to UV or chemical disinfectants.[205]	Not widely available. Effectiveness depends on surface properties.[205]

[a]It is important to ensure that the choice of disinfectant is safe and compatible with the substrate it is applied to. *NFPA rating specified as [health, flammability, instability].

https://doi.org/10.1021/acsomega.0c06335
ACS Omega 2021, 6, 6509−6527

Chemical disinfectants have been evaluated for their ability to inactivate various types of coronaviruses.[27,84] For SARS-CoV-2, suspension tests showed >3 $\log_{10}$ $TCID_{50}$/mL reduction in virus titer within 5 min at room temperature using 1, 2, and 10% household bleach (sodium hypochlorite), 70% ethanol, 7.5% povidone-iodine, 0.05% chloroxylenol, 0.05% chlorhexidine, and 0.1% benzalkonium chloride.[84,160] For other coronaviruses (e.g., SARS-CoV-1, MERS-CoV, and MHV), suspension tests showed >4 $\log_{10}$ reduction in virus titer within 30 s using 78, 80, 85, and 95% ethanol,[161−163] 75% 2-propanol,[162] a mixture of 45% 2-propanol and 30% 1-propanol,[163] and 1, 4, and 7.5% povidone-iodine.[164]

For SARS-CoV-2, carrier tests performed on glass surfaces showed >3 $\log_{10}$ and >4 $\log_{10}$ reduction in virus titer within 2 min using disinfectant wipes containing 0.19% benzalkonium chloride and a spray mixture of 50% ethanol and 0.083% alkyl (50% C14, 40% C12, and 10% C16) dimethyl benzyl ammonium saccharinate, respectively.[165] Carrier tests performed on stainless steel disks showed >3 $\log_{10}$ reduction within 1 min for HCoV-229E, MHV, and TGEV exposed to 70% ethanol[41,166] and for HCoV-229E exposed to 0.1 and 0.5% sodium hypochlorite and 2% glutaraldehyde.[166] In another study, hydrogen peroxide vapor inactivated TGEV in a carrier test by a reduction of >4 $\log_{10}$, but it took 2−3 h to do so.[167] Prior carrier tests have been performed primarily on stainless steel. Results using stainless steel carriers may not reflect disinfectant effectiveness on other fomites with different surface properties (e.g., surface chemistry, wettability, porosity, and roughness). The dependence of disinfectant effectiveness on surface properties remains an open question and is an area for further research.

5.2.2. Ultraviolet (UV) and Solar Irradiation. UVC irradiation (100−280 nm; typically 254 nm is used) damages nucleic acid bases in the genetic material and, to a lesser extent, proteins in virus capsids.[83,148] UVC irradiation induces dimerization of adjacent uracil bases in RNA, forming pyrimidine dimers that disrupt the RNA structure, which inhibits the viral replication process and inactivates the virus.[83,168] Exposure of SARS-CoV-1 to a UVC light source (254 nm, ∼1446 mJ/cm^2) held 3 cm above the virus resulted in a ∼ 4.5 $\log_{10}$ $TCID_{50}$/mL reduction in virus titer within 6 min. Exposure to other UV wavelengths (e.g., UVA) was found to be insufficient to inactivate the virus.[169] UV doses of 500−1800 mJ/cm^2 resulted in 99.9% inactivation in viruses tested (including MERS-CoV, SARS-CoV, influenza A, and MS2 bacteriophage).[170]

UVC irradiation as a disinfection strategy poses a few challenges. The time required to inactivate SARS-CoV-1 using UVC (254 nm, ∼1446 mJ/cm^2), ∼6 min at 4016 μW/cm^2, is significantly longer than the time required using chemical disinfectants (30 s to 1 min).[27,169] This time to inactivate only applies to regions of an object directly exposed to UVC irradiation. Disinfectant effectiveness reduces significantly in shadowed regions. Additionally, UVC radiation may pose health risks, including skin cancer and ocular damage to exposed individuals.[171] Nonetheless, UVC-based disinfection can be valuable for use in applications where the irradiation can be shielded from humans, and it has been used in, for example, empty buses and other vehicles.[12]

Recent studies have quantified the rate of SARS-CoV-2 inactivation using UV radiation. Exposure of SARS-CoV-2 to a UVC light source (254 nm, 1048 mJ/cm^2) held 3 cm above the virus resulted in a >4 $\log_{10}$ $TCID_{50}$/mL reduction in virus titer within 6 min, and "complete inactivation" (>6 $\log_{10}$ $TCID_{50}$/mL) within 9 min.[172] In another study, a pulsed-xenon ultraviolet (PX-UV) system was tested for its efficacy in inactivating SARS-CoV-2 that had been dried on hard (cell culture chamber slides) and soft (N95 respirators) surfaces as carriers. Exposure of the virus to PX-UV on the hard surface resulted in >3.5 $\log_{10}$ PFU/mL reduction within 1 min and >4 $\log_{10}$ PFU/mL reduction within 2 min. On the soft surface, 5 min of exposure to PX-UV resulted in >4.5 $\log_{10}$ PFU/mL reduction.[173]

The inactivation of viruses by solar irradiation has also been studied, especially in the context of the disinfection of water. The range of UV wavelengths in sunlight that reach the surface of Earth is between 290 and 400 nm because UVC is typically completely blocked by the atmosphere.[168,174] The antiviral properties of sunlight primarily come from UVB light, which can also form pyrimidine dimers, but these mechanisms are not as well studied as the mechanisms of UVC-based disinfection.[168] Additionally, the solar spectrum, especially in the UV wavelengths, can vary significantly depending on environmental factors, the time of day, and the season. Such factors can lead to large variations in the efficiency of virus inactivation by sunlight.[168]

5.2.3. Heat Treatment. Heat treatment is a well-known method for disinfecting surfaces. At temperatures exceeding ∼80 °C, viral capsid proteins are denatured and RNA is damaged.[83] SARS-CoV-2 has been shown to become inactivated within 5 min at 70 °C in a suspension test, with a reduction from an initial concentration of ∼6.8 $\log_{10}$ $TCID_{50}$/mL to ∼2 $\log_{10}$ $TCID_{50}$/mL.[84] Carrier tests performed by heating SARS-CoV-2 on N95 masks and stainless steel to 70 °C show that it can take ∼50 min and >100 min, respectively, for a reduction from an initial concentration of ∼4 $\log_{10}$ $TCID_{50}$/mL to ∼0.5 $\log_{10}$ $TCID_{50}$/mL.[147] Sufficiently high temperatures and exposure times should be used. Moderately high temperatures (19−37 °C) only cause minor damage to the protein capsid and fail to inactivate some viruses.[83]

Autoclave is a common method of sterilizing equipment using heat treatment in a laboratory or clinical environment. Autoclaves produce steam at high temperatures (∼132 °C) in a pressurized chamber. At this temperature, most microbes, including viruses, are inactivated. In one experiment, avian coronavirus and avian pneumovirus carried by cotton swabs were inactivated after heat treatment using an autoclave for 20 min. In the same study, heating the same viruses in a microwave oven for 5 s was also found to be sufficient for inactivation.[175]

5.3. Emerging Disinfection Technologies. This section summarizes emerging technologies for the inactivation of virus particles, including SARS-CoV-2.

5.3.1. Self-Disinfecting Materials and Surfaces. Engineering self-disinfecting surfaces is an emerging avenue of research for preventing infection transmission by fomites. While certain materials like copper and silver have long been known to possess intrinsic antimicrobial properties, various types of surface modification and functionalization can also give rise to antimicrobial properties against bacteria and viruses.[126,127] Only a limited number of works have focused on virus-specific self-disinfection.[128] This section highlights some of these studies. Readers are referred to a recent review for details.[129]

Copper and silver alloys are known viricidal agents that inactivate viruses through multiple modes of action. The

https://doi.org/10.1021/acsomega.0c06335
ACS Omega 2021, 6, 6509−6527

primary mechanism involves direct interaction between metal ions and microbial proteins or indirect interaction through the formation of radicals that are damaging to DNA and lipid membranes.[130,131] Copper has been shown to retain its effectiveness across a range of humidities and temperatures, while silver had drastically reduced antimicrobial effectiveness at low humidities (~20% RH).[176]

Pure copper and alloys with 79−89% copper were found to be the most effective in inactivating viruses. Abrasion and removal of the outer oxide layer caused a slight decrease in effectiveness. In one study, 5×10^5 PFU/cm^2 nonenveloped murine norovirus was inactivated under 2 h at room temperature.[185] Inactivation of norovirus by copper was found to be up to 10× faster in dry conditions than in wet conditions, but the mechanisms underlying such differences were unclear.[186] In another study, copper yielded a near 4-log reduction in enveloped influenza A virus particle count after 6 h.[187] Table 3 includes the effectiveness of copper on some coronaviruses in lowering viability periods. Some studies examining the clinical effectiveness of copper surfaces have shown notable improvement toward infection control benchmarks with 94% less bacteria when compared with control plastic surfaces on ICU beds.[188]

Photocatalytic action has been shown to be highly effective in inactivating numerous enveloped and nonenveloped viruses by damaging DNA and lipid membranes via the photocatalyzed formation of hydroxyl radicals in the presence of photoactive oxides.[189,190] Titanium dioxide (TiO_2) is a popular photocatalytic material due to its long lifetime and effectiveness over a wide range of microbes. TiO_2 has the potential to provide antiviral protection to a range of materials. Cotton fabrics have been impregnated with TiO_2 via magnesium nanoparticle carriers.[191] TiO_2 impregnated into resin, fiberglass, and PVC have also been used to coat various surfaces in hospitals, schools, and other public places.[192]

Despite the potentials that self-disinfecting surfaces present, their widespread adoption, especially in hospitals, has been limited by a lack of clinical data characterizing their effectiveness over time and the cost of retrofitting and upgrading existing equipment.[193]

5.3.2. Plasma Disinfection. Plasma is an ionized gas made up of charged and uncharged particles (i.e., ions and electrons and molecules and atoms, respectively), reactive species, and UV photons.[194,195] Plasma can be thermal or nonthermal depending on whether electrons are at the same or higher temperature as heavy particles. Cold atmospheric plasma (CAP) is a low-temperature, nonthermal plasma that is produced by a variety of methods using gases such as helium, argon, nitrogen, heliox, and/or air. Two common methods for producing CAP are dielectric barrier discharge and atmospheric pressure plasma jet.[194]

CAP is an emerging disinfection technology that has been considered for applications in dentistry and oncology and in food processing.[194,195] The antimicrobial properties of CAP are attributed to reactive oxygen and nitrogen species generated in the nonthermal plasma.[195,206,207] Although the details of the inactivation mechanisms are still under investigation, it is believed that the reactive species damage the genetic material and proteins.[208] In one study, singlet oxygen in plasma was implicated in the inactivation of bacteriophages through multiple mechanisms involving reactions with amino acids and DNA nucleotide oxidation and cross-linking, but the primary mechanism was thought to be singlet oxygen-induced cross-linking of capsid proteins.[208]

Recently, CAP with argon feed gas was shown to cause a >3 $\log_{10}$ $TCID_{50}$/mL reduction in SARS-CoV-2 titer on plastic, metal, cardboard, a basketball, and various leathers within 3 min. The effectiveness of inactivation primarily depended on surface roughness and absorptivity. These results are very promising as CAP can be a safer alternative to traditional disinfection techniques such as UV and chemical disinfectants.[205]

5.4. Hand Hygiene. Frequent handwashing can lower the incidence of transfer from fomites to facial membranes via contact.[209] Considering the frequency with which adults touch their faces (23 times per hour) and the risk of infection that is associated with face touching, handwashing is a critically important personal hygiene habit.[67]

Handwashing is effective in reducing the spread of a virus from hands by reducing any present viral load.[209,210] Furthermore, recently washed hands that are subsequently contaminated with virus particles were found to transfer less of those particles to touched surfaces.[113] However, handwashing is only as effective as the frequency, the effectiveness of the antiseptic, and thoroughness.[210] The CDC recommends washing for a minimum of 20 s.[211] This recommendation was based on a few empirical studies,[212−214] including one that investigated handwashing practices such as wash time (15 s vs 30 s) and the effect of soiled hands on infectivity reduction.[215]

To evaluate the effectiveness of a handwashing, a fingerpad method is typically used.[216,217] Here, a virus is inoculated on precleaned fingerpads, allowed to dry, and then subjected to exposure to an antiseptic by static contact with the fingerpad.[218,219] The ASTM specifies that an effective handwashing antiseptic must yield a minimum reduction of 4 $\log_{10}$ (99.99%) in virus titer from the initial inoculation titer. However, this standard does not specify a minimum contact time between the fingerpad and the antiseptic.[220] Another potential drawback of these standard tests is that they may not be representative of *in vivo* handwashing behavior of healthcare workers or the general public.[217]

Viruses present a unique challenge for handwashing in that their structure and ability to survive on the skin may evade inactivation by handwashing methods customized for bacterial disinfection.[209] Alcohol- and isopropanol-based antiseptics (60−80% ethanol) are the most effective nonhazardous antiseptic, especially against enveloped viruses.[221] Other WHO-recommended antiviral antiseptics (from the most to the least effective) are iodophors (0.5−10%), chlorhexidine (0.5−4%), and chloroxylenol (0.5−4%), but it should be noted that all of these are less effective than alcohol.[221] In regard to hand sanitizers, SARS-CoV-1 has been confirmed to be the most susceptible to ethanol and isopropanol using suspension tests with 1 part virus at 10^7 $TCID_{50}$/mL, 1 part media, and 8 parts by volume of an ethanol- or isopropanol-based WHO-recommended antiseptic formulation. A >4 $\log_{10}$ SARS-CoV-1 reduction was achieved in 30 s using ethanol and isopropanol formulations at 80 and 75% concentrations, respectively, and using dilutions as low as 40%.[162,221]

6. CONCLUSIONS

The COVID-19 pandemic has revealed major gaps in our scientific knowledge, not only of the biology of how the virus infects humans but also of the role of physicochemical processes and surface science involved. Due to the incomplete

https://doi.org/10.1021/acsomega.0c06335
ACS Omega 2021, 6, 6509−6527

understanding of the adsorption and transfer properties of viruses including SARS-CoV-2, as well as challenges in sampling and quantifying infective viruses from surfaces, it is difficult to fully determine the contribution of fomite transmission compared with other routes of transmission. While RT-PCR and cell culture assays are commonly used to detect viruses, they are slow and require access to the established laboratory infrastructure. It is difficult, therefore, to apply them broadly for rapid virus tracking (e.g., in highly trafficked public areas) and for predicting the onset of an outbreak. It is also difficult to verify whether surface disinfection is successful, which is important for common or public spaces that are frequently used (e.g., public bathrooms and public transportation).

Table 6 lists some of the open questions we have identified. Addressing these questions will allow us to devise more effective strategies to combat the spread of the disease. For example, quantitative models predicting the locations of high-risk areas within a building and high-risk objects within those areas can inform the prioritization for disinfection. A better understanding of disinfectant effectiveness on different surfaces and their potential side effects, such as their toxicity and negative impact on human health and the environment (see Table 5), allows one to choose the optimal disinfection strategy for specific applications. The identification of surfaces with high contamination risk also presents an opportunity for self-cleaning communal surfaces such as water faucets or door handles. With improved understanding of the physicochemical origins of virus adsorption, it may be possible to devise novel disinfection strategies that are based on the modification of virus−surface XDLVO interactions to prevent virus adsorption in the first place,[222] rather than inactivating viruses already deposited on a surface, a principle that most common disinfectants rely on. While our review is by no means exhaustive, we hope that it provides a starting point for researchers in the physical sciences interested in COVID-19 for taking on some of the open research challenges so that as a community, we can be better prepared for the next pandemic.

Table 6. Open Questions on Transmission and Disinfection of SARS-CoV-2[a]

fomite transmission
•What is the infectivity of the fomite transmission route compared with other routes?
•What is the adhesion and transfer efficiency of SARS-CoV-2 between human skins and different surfaces?
•How can we better quantify and predict how surface properties of the virus and surfaces influence the adhesion, transfer, and persistence characteristics?
•How can infective viruses be detected more quickly (less than a few hours) than current methods?
•How can we better predict the locations and objects that are at high risk of virus contamination and design tools to mitigate this risk?
surface disinfection
•How can one better predict the rate of virus inactivation based on its structure and composition?
•How do the surface properties (e.g., roughness, porosity, wettability, and presence of impurities) alter disinfectant effectiveness?
•What is the optimal disinfection strategy to maximize disinfection effectiveness but minimize side effects, including health hazards, pollution, and damage to surfaces?
•What innovations are needed for self-disinfecting surface technologies to be adopted broadly?

[a]A number of questions are also applicable to other viruses.

AUTHOR INFORMATION

Corresponding Author

Sindy K. Y. Tang − *Department of Mechanical Engineering, Stanford University, Stanford, California 94305, United States*; orcid.org/0000-0003-1465-2432; Email: sindy@stanford.edu

Authors

Nicolas Castaño − *Department of Mechanical Engineering, Stanford University, Stanford, California 94305, United States*

Seth C. Cordts − *Department of Mechanical Engineering, Stanford University, Stanford, California 94305, United States*

Myra Kurosu Jalil − *Department of Mechanical Engineering, Stanford University, Stanford, California 94305, United States*

Kevin S. Zhang − *Department of Mechanical Engineering, Stanford University, Stanford, California 94305, United States*

Saisneha Koppaka − *Department of Mechanical Engineering, Stanford University, Stanford, California 94305, United States*

Alison D. Bick − *Department of Mechanical Engineering, Stanford University, Stanford, California 94305, United States*

Rajorshi Paul − *Department of Mechanical Engineering, Stanford University, Stanford, California 94305, United States*

Complete contact information is available at: https://pubs.acs.org/10.1021/acsomega.0c06335

Author Contributions

‡N.C., S.C.C., M.K.J., and K.S.Z. contributed equally to this work. The manuscript was written through contributions of all authors. All authors have given approval to the final version of the manuscript.

Funding

This work is supported by the National Science Foundation (award #2030390).

Notes

The authors declare no competing financial interest.

REFERENCES

(1) Johns Hopkins University. COVID-19 Dashboard https://coronavirus.jhu.edu/ (accessed Dec 28, 2020).

(2) NIH. COVID-19, MERS & SARS https://www.niaid.nih.gov/diseases-conditions/covid-19 (accessed Apr 11, 2020).

(3) Kutter, J. S.; Spronken, M. I.; Fraaij, P. L.; Fouchier, R. A.; Herfst, S. Transmission routes of respiratory viruses among humans. *Curr. Opin. Virol.* **2018**, *28*, 142−151.

(4) Boone, S. A.; Gerba, C. P. Significance of fomites in the spread of respiratory and enteric viral disease. *Appl. Environ. Microbiol.* **2007**, *73*, 1687−1696.

(5) Cai, J.; Sun, W.; Huang, J.; Gamber, M.; Wu, J.; He, G. Indirect Virus Transmission in Cluster of COVID-19 Cases, Wenzhou, China, 2020. *Emerging Infect. Dis.* **2020**, *26*, 1343−1345.

(6) Galbadage, T.; Peterson, B. M.; Gunasekera, R. S. Does COVID-19 Spread Through Droplets Alone? *Front. Public Health* **2020**, *8*, 163.

(7) Joonaki, E.; Hassanpouryouzband, A.; Heldt, C. L.; Areo, O. Surface Chemistry Can Unlock Drivers of Surface Stability of SARS-CoV-2 in a Variety of Environmental Conditions. *Chem* **2020**, *6*, 2135−2146.

https://doi.org/10.1021/acsomega.0c06335
ACS Omega 2021, 6, 6509−6527

(8) Stephens, B.; Azimi, P.; Thoemmes, M. S.; Heidarinejad, M.; Allen, J. G.; Gilbert, J. A. Microbial exchange via fomites and implications for human health. *Curr. Pollution Rep.* **2019**, 198.
(9) Taylor, A. Large-Scale Disinfection Efforts Against Coronavirus. https://www.theatlantic.com/photo/2020/03/photos-large-scale-disinfection-efforts-against-coronavirus/607810/ (accessed Apr 11, 2020).
(10) Nasrallah, T. Dubai Municipality continues campaign to disinfect public facilities. https://gulfnews.com/uae/dubai-municipality-continues-campaign-to-disinfect-public-facilities-1.1585420891506 (accessed Apr 11, 2020).
(11) Yang, J. 3 ways China is using drones to fight coronavirus. https://www.weforum.org/agenda/2020/03/three-ways-china-is-using-drones-to-fight-coronavirus/ (accessed Apr 11, 2020).
(12) Sustainable Bus. Bus disinfection through UV lights: A way to fight Coronavirus in Shanghai. https://www.sustainable-bus.com/news/bus-disinfection-through-uv-lights-a-way-to-fight-coronavirus-in-shanghai/ (accessed May 10, 2020).
(13) Schoeman, D.; Fielding, B. C. Coronavirus envelope protein: current knowledge. *Virol. J.* **2019**, *16*, 69.
(14) de Haan, C. A.; Vennema, H.; Rottier, P. J. Assembly of the coronavirus envelope: homotypic interactions between the M proteins. *J. Virol.* **2000**, *74*, 4967−4978.
(15) Walls, A. C.; Park, Y.-J.; Tortorici, M. A.; Wall, A.; McGuire, A. T.; Veesler, D. Structure, Function, and Antigenicity of the SARS-CoV-2 Spike Glycoprotein. *Cell* **2020**, *181*, 281−292.e6.
(16) Gelderblom, H. R. Structure and classification of viruses. In *Medical Microbiology*; Baron, S., Ed.; University of Texas Medical Branch at Galveston: Galveston (TX), 1996.
(17) Vollenbroich, D.; Özel, M.; Vater, J.; Kamp, R. M.; Pauli, G. Mechanism of inactivation of enveloped viruses by the biosurfactant surfactin from Bacillus subtilis. *Biologicals* **1997**, *25*, 289−297.
(18) Lucas, W. Viral capsids and envelopes: structure and function. In *Encyclopedia of life sciences*; John Wiley & Sons, Ltd: Chichester, UK, 2001.
(19) Wrapp, D.; Wang, N.; Corbett, K. S.; Goldsmith, J. A.; Hsieh, C.-L.; Abiona, O.; Graham, B. S.; McLellan, J. S. Cryo-EM structure of the 2019-nCoV spike in the prefusion conformation. *Science* **2020**, *367*, 1260−1263.
(20) Yan, R.; Zhang, Y.; Li, Y.; Xia, L.; Guo, Y.; Zhou, Q. Structural basis for the recognition of SARS-CoV-2 by full-length human ACE2. *Science* **2020**, *367*, 1444−1448.
(21) Karimzadeh, S.; Bhopal, R.; Tien, H. N. Review of viral dynamics, exposure, infective dose, and outcome of COVID-19 caused bythe SARS-COV2 virus: comparison with other respiratory viruses. 2020, Preprints. https://www.preprints.org/manuscript/202007.0613/v1.
(22) Pfefferle, S.; Guenther, T.; Kobbe, R.; Czech-Sioli, M.; Noerz, D.; Santer, R.; Oh, J.; Kluge, S.; Oestereich, L.; Peldschus, K.; et al. Low and high infection dose transmission of SARS-CoV-2 in the first COVID-19 clusters in Northern Germany. 2020, medRxiv. https://www.medrxiv.org/content/10.1101/2020.06.11.20127332v1.
(23) Evans, M. Avoiding COVID-19: Aerosol Guidelines. 2020, medRxiv. https://www.medrxiv.org/content/10.1101/2020.05.21.20108894v3.
(24) Hu, B.; Guo, H.; Zhou, P.; Shi, Z.-L. Characteristics of SARS-CoV-2 and COVID-19. *Nat. Rev. Microbiol.* **2020**, 141.
(25) Blair, R. V.; Vaccari, M.; Doyle-Meyers, L. A.; Roy, C. J.; Russell-Lodrigue, K.; Fahlberg, M.; Monjure, C. J.; Beddingfield, B.; Plante, K. S.; Plante, J. A.; et al. ARDS and Cytokine Storm in SARS-CoV-2 Infected Caribbean Vervets. 2020, BioRxiv. https://www.biorxiv.org/content/10.1101/2020.06.18.157933v2.
(26) Watanabe, T.; Bartrand, T. A.; Weir, M. H.; Omura, T.; Haas, C. N. Development of a dose-response model for SARS coronavirus. *Risk Anal.* **2010**, *30*, 1129−1138.
(27) Kampf, G.; Todt, D.; Pfaender, S.; Steinmann, E. Persistence of coronaviruses on inanimate surfaces and their inactivation with biocidal agents. *J. Hosp. Infect.* **2020**, *104*, 246−251.
(28) Yao, H.; Song, Y.; Chen, Y.; Wu, N.; Xu, J.; Sun, C.; Zhang, J.; Weng, T.; Zhang, Z.; Wu, Z.; et al. Molecular Architecture of the SARS-CoV-2 Virus. *Cell* **2020**, *183*, 730−738.
(29) Verma, S.; Bednar, V.; Blount, A.; Hogue, B. G. Identification of functionally important negatively charged residues in the carboxy end of mouse hepatitis coronavirus A59 nucleocapsid protein. *J. Virol.* **2006**, *80*, 4344−4355.
(30) Hu, Y.; Wen, J.; Tang, L.; Zhang, H.; Zhang, X.; Li, Y.; Wang, J.; Han, Y.; Li, G.; Shi, J.; et al. The M protein of SARS-CoV: basic structural and immunological properties. *Genomics Proteomics Bioinformatics* **2003**, *1*, 118−130.
(31) Laude, H.; Masters, P. S. The coronavirus nucleocapsid protein. In *The Coronaviridae*; Siddell, S. G., Ed.; Springer US: Boston, MA, 1995; pp. 141−163, DOI: 10.1007/978-1-4899-1531-3_7.
(32) Mi, X.; Bromley, E. K.; Joshi, P. U.; Long, F.; Heldt, C. L. Virus Isoelectric Point Determination Using Single-Particle Chemical Force Microscopy. *Langmuir* **2020**, *36*, 370−378.
(33) Mayer, B. K.; Yang, Y.; Gerrity, D. W.; Abbaszadegan, M. The impact of capsid proteins on virus removal and inactivation during water treatment processes. *Microbiol. Insights* **2015**, *8*, 15−28.
(34) WHO. *Laboratory biosafety guidance related to the novel coronavirus (2019 - nCoV)*; World Health Organization: 2020.
(35) Millet, J. K.; Tang, T.; Nathan, L.; Jaimes, J. A.; Hsu, H.-L.; Daniel, S.; Whittaker, G. R. Production of pseudotyped particles to study highly pathogenic coronaviruses in a biosafety level 2 setting. *J. Visualized Exp.* **2019**, No. e59010.
(36) Giroglou, T.; Cinatl, J.; Rabenau, H.; Drosten, C.; Schwalbe, H.; Doerr, H. W.; von Laer, D. Retroviral vectors pseudotyped with severe acute respiratory syndrome coronavirus S protein. *J. Virol.* **2004**, *78*, 9007−9015.
(37) Moore, M. J.; Dorfman, T.; Li, W.; Wong, S. K.; Li, Y.; Kuhn, J. H.; Coderre, J.; Vasilieva, N.; Han, Z.; Greenough, T. C.; et al. Retroviruses pseudotyped with the severe acute respiratory syndrome coronavirus spike protein efficiently infect cells expressing angiotensin-converting enzyme 2. *J. Virol.* **2004**, *78*, 10628−10635.
(38) Ou, X.; Liu, Y.; Lei, X.; Li, P.; Mi, D.; Ren, L.; Guo, L.; Guo, R.; Chen, T.; Hu, J.; et al. Characterization of spike glycoprotein of SARS-CoV-2 on virus entry and its immune cross-reactivity with SARS-CoV. *Nat. Commun.* **2020**, *11*, 1620.
(39) Casanova, L.; Rutala, W. A.; Weber, D. J.; Sobsey, M. D. Survival of surrogate coronaviruses in water. *Water Res.* **2009**, *43*, 1893−1898.
(40) Casanova, L. M.; Jeon, S.; Rutala, W. A.; Weber, D. J.; Sobsey, M. D. Effects of air temperature and relative humidity on coronavirus survival on surfaces. *Appl. Environ. Microbiol.* **2010**, *76*, 2712−2717.
(41) Hulkower, R. L.; Casanova, L. M.; Rutala, W. A.; Weber, D. J.; Sobsey, M. D. Inactivation of surrogate coronaviruses on hard surfaces by health care germicides. *Am. J. Infect. Control* **2011**, *39*, 401−407.
(42) Zhao, S.; Gao, J.; Zhu, L.; Yang, Q. Transmissible gastroenteritis virus and porcine epidemic diarrhoea virus infection induces dramatic changes in the tight junctions and microfilaments of polarized IPEC-J2 cells. *Virus Res.* **2014**, *192*, 34−45.
(43) Kim, Y.; Krishna, V. D.; Torremorell, M.; Goyal, S. M.; Cheeran, M. C.-J. Stability of porcine epidemic diarrhea virus on fomite materials at different temperatures. *Vet. Sci.* 2018, *5*, DOI: 10.3390/vetsci5010021.
(44) Schneider, M.; Ackermann, K.; Stuart, M.; Wex, C.; Protzer, U.; Schätzl, H. M.; Gilch, S. Severe acute respiratory syndrome coronavirus replication is severely impaired by MG132 due to proteasome-independent inhibition of M-calpain. *J. Virol.* **2012**, *86*, 10112−10122.
(45) Pratelli, A. Canine coronavirus inactivation with physical and chemical agents. *Vet. J.* **2008**, *177*, 71−79.
(46) Pratelli, A. Action of disinfectants on canine coronavirus replication in vitro. *Zoonoses Public Health* **2007**, *54*, 383−386.
(47) Prussin, A. J.; Schwake, D. O.; Lin, K.; Gallagher, D. L.; Buttling, L.; Marr, L. C. Survival of the enveloped virus phi6 in droplets as a function of relative humidity, absolute humidity, and temperature. *Appl. Environ. Microbiol.* **2018**, *84*, No. e00551-18.

(48) Woolwine, J. D.; Gerberding, J. L. Effect of testing method on apparent activities of antiviral disinfectants and antiseptics. *Antimicrob. Agents Chemother.* **1995**, *39*, 921−923.
(49) Gallandat, K.; Wolfe, M. K.; Lantagne, D. Surface Cleaning and Disinfection: Efficacy Assessment of Four Chlorine Types Using Escherichia coli and the Ebola Surrogate Phi6. *Environ. Sci. Technol.* **2017**, *51*, 4624−4631.
(50) Pitol, A. K.; Bischel, H. N.; Kohn, T.; Julian, T. R. Virus Transfer at the Skin-Liquid Interface. *Environ. Sci. Technol.* **2017**, *51*, 14417−14425.
(51) De Santis, E.; Alkassem, H.; Lamarre, B.; Faruqui, N.; Bella, A.; Noble, J. E.; Micale, N.; Ray, S.; Burns, J. R.; Yon, A. R.; et al. Antimicrobial peptide capsids of de novo design. *Nat. Commun.* **2017**, *8*, 2263.
(52) Zuo, Y. Y.; Uspal, W. E.; Wei, T. Airborne Transmission of COVID-19: Aerosol Dispersion, Lung Deposition, and Virus-Receptor Interactions. *ACS Nano* **2020**, *16*, 16502.
(53) Li, Q.; Guan, X.; Wu, P.; Wang, X.; Zhou, L.; Tong, Y.; Ren, R.; Leung, K. S. M.; Lau, E. H. Y.; Wong, J. Y.; et al. Early Transmission Dynamics in Wuhan, China, of Novel Coronavirus-Infected Pneumonia. *N. Engl. J. Med.* **2020**, *382*, 1199−1207.
(54) Richard, M.; Knauf, S.; Lawrence, P.; Mather, A. E.; Munster, V. J.; Müller, M. A.; Smith, D.; Kuiken, T. Factors determining human-to-human transmissibility of zoonotic pathogens via contact. *Curr. Opin. Virol.* **2017**, *22*, 7−12.
(55) Gralton, J.; Tovey, E.; McLaws, M.-L.; Rawlinson, W. D. The role of particle size in aerosolised pathogen transmission: a review. *J. Infect.* **2011**, *62*, 1−13.
(56) Tellier, R.; Li, Y.; Cowling, B. J.; Tang, J. W. Recognition of aerosol transmission of infectious agents: a commentary. *BMC Infect. Dis.* **2019**, *19*, 101.
(57) Asadi, S.; Cappa, C. D.; Barreda, S.; Wexler, A. S.; Bouvier, N. M.; Ristenpart, W. D. Efficacy of masks and face coverings in controlling outward aerosol particle emission from expiratory activities. *Sci. Rep.* **2020**, *10*, 15665.
(58) Wells, W. F. On air-borne infection. *Am. J. Epidemiol.* **1934**, *20*, 611−618.
(59) Xie, X.; Li, Y.; Chwang, A. T. Y.; Ho, P. L.; Seto, W. H. How far droplets can move in indoor environments–revisiting the Wells evaporation-falling curve. *Indoor Air* **2007**, *17*, 211−225.
(60) Bourouiba, L.; Dehandschoewercker, E.; Bush, J. W. Violent expiratory events: on coughing and sneezing. *J. Fluid Mech.* **2014**, *745*, 537−563.
(61) Bourouiba, L. Turbulent Gas Clouds and Respiratory Pathogen Emissions: Potential Implications for Reducing Transmission of COVID-19. *JAMA* **2020**, *323*, 1837−1838.
(62) Beggs, C. B. Is there an airborne component to the transmission of COVID-19? : a quantitative analysis study. 2020, medRxiv. https://www.medrxiv.org/content/10.1101/2020.05.22.20109991v2.
(63) Fennelly, K. P. Particle sizes of infectious aerosols: implications for infection control. *Lancet Respir. Med.* **2020**, *8*, 914−924.
(64) Samet, J. M.; Prather, K.; Benjamin, G.; Lakdawala, S.; Lowe, J.-M.; Reingold, A.; Volckens, J.; Marr, L. C. Airborne Transmission of SARS-CoV-2: What We Know. *Clin. Infect. Dis.* **2021**, ciab039.
(65) Prather, K. A.; Marr, L. C.; Schooley, R. T.; McDiarmid, M. A.; Wilson, M. E.; Milton, D. K. Airborne transmission of SARS-CoV-2. *Science* **2020**, *370*, 303−304.
(66) Ong, S. W. X.; Tan, Y. K.; Chia, P. Y.; Lee, T. H.; Ng, O. T.; Wong, M. S. Y.; Marimuthu, K. Air, Surface Environmental, and Personal Protective Equipment Contamination by Severe Acute Respiratory Syndrome Coronavirus 2 (SARS-CoV-2) From a Symptomatic Patient. *JAMA* **2020**, *323*, 1610−1612.
(67) Kwok, Y. L. A.; Gralton, J.; McLaws, M.-L. Face touching: a frequent habit that has implications for hand hygiene. *Am. J. Infect. Control* **2015**, *43*, 112−114.
(68) Edward, D. G. Resistance of influenza virus to drying and its demonstration on dust. *Lancet* **1941**, *238*, 664−666.
(69) Asadi, S.; ben Hnia, N. G.; Barre, R. S.; Wexler, A. S.; Ristenpart, W. D.; Bouvier, N. M. Influenza A virus is transmissible via aerosolized fomites. *Nat. Commun.* **2020**, *11*, 1−9.
(70) Wang, W.; Xu, Y.; Gao, R.; Lu, R.; Han, K.; Wu, G.; Tan, W. Detection of SARS-CoV-2 in Different Types of Clinical Specimens. *JAMA* **2020**, *323*, 1843−1844.
(71) Wang, X. W.; Li, J.; Guo, T.; Zhen, B.; Kong, Q.; Yi, B.; Li, Z.; Song, N.; Jin, M.; Xiao, W.; et al. Concentration and detection of SARS coronavirus in sewage from Xiao Tang Shan Hospital and the 309th Hospital of the Chinese People's Liberation Army. *Water Sci. Technol.* **2005**, *52*, 213−221.
(72) Medema, G.; Heijnen, L.; Elsinga, G.; Italiaander, R.; Brouwer, A. Presence of SARS-Coronavirus-2 RNA in Sewage and Correlation with Reported COVID-19 Prevalence in the Early Stage of the Epidemic in The Netherlands. *Environ. Sci. Technol. Lett.* **2020**, *7*, 511.
(73) *Pesticide Application Methods*; Matthews, G. A., Ed.; Blackwell Science Ltd.: Oxford, UK, 2000.
(74) Nicas, M. Markov modeling of contaminant concentrations in indoor air. *Am. Ind. Hyg. Assoc. J.* **2000**, *61*, 484−491.
(75) Nicas, M.; Jones, R. M. Relative contributions of four exposure pathways to influenza infection risk. *Risk Anal.* **2009**, *29*, 1292−1303.
(76) Verreault, D.; Moineau, S.; Duchaine, C. Methods for sampling of airborne viruses. *Microbiol. Mol. Biol. Rev.* **2008**, *72*, 413−444.
(77) Kwon, H.-J.; Fronczek, C. F.; Angus, S. V.; Nicolini, A. M.; Yoon, J.-Y. Rapid and Sensitive Detection of H1N1/2009 Virus from Aerosol Samples with a Microfluidic Immunosensor. *J. Lab. Autom.* **2014**, *19*, 322−331.
(78) Damit, B. Droplet-based microfluidics detector for bioaerosol detection. *Aerosol Sci. Technol.* **2017**, *51*, 488−500.
(79) Yeh, Y.-T.; Gulino, K.; Zhang, Y.; Sabestien, A.; Chou, T.-W.; Zhou, B.; Lin, Z.; Albert, I.; Lu, H.; Swaminathan, V.; et al. A rapid and label-free platform for virus capture and identification from clinical samples. *Proc. Natl. Acad. Sci. U. S. A.* **2020**, *117*, 895−901.
(80) Harvey, A. P.; Fuhrmeister, E. R.; Cantrell, M. E.; Pitol, A. K.; Swarthout, J. M.; Powers, J. E.; Nadimpalli, M. L.; Julian, T. R.; Pickering, A. J. Longitudinal Monitoring of SARS-CoV-2 RNA on High-Touch Surfaces in a Community Setting. *Environ. Sci. Technol. Lett.* **2020**, *8*, 168.
(81) Julian, T. R.; Tamayo, F. J.; Leckie, J. O.; Boehm, A. B. Comparison of surface sampling methods for virus recovery from fomites. *Appl. Environ. Microbiol.* **2011**, *77*, 6918−6925.
(82) Taku, A.; Gulati, B. R.; Allwood, P. B.; Palazzi, K.; Hedberg, C. W.; Goyal, S. M. Concentration and detection of caliciviruses from food contact surfaces. *J. Food Prot.* **2002**, *65*, 999−1004.
(83) Zhang, Y.; Qu, S.; Xu, L. Progress in the study of virus detection methods: The possibility of alternative methods to validate virus inactivation. *Biotechnol. Bioeng.* **2019**, *116*, 2095−2102.
(84) Chin, A. W. H.; Chu, J. T. S.; Perera, M. R. A.; Hui, K. P. Y.; Yen, H.-L.; Chan, M. C. W.; Peiris, M.; Poon, L. L. M. Stability of SARS-CoV-2 in different environmental conditions. *Lancet Microbe* **2020**, *1*, No. e10.
(85) Matsuyama, S.; Nao, N.; Shirato, K.; Kawase, M.; Saito, S.; Takayama, I.; Nagata, N.; Sekizuka, T.; Katoh, H.; Kato, F.; et al. Enhanced isolation of SARS-CoV-2 by TMPRSS2-expressing cells. *Proc. Natl. Acad. Sci. U. S. A.* **2020**, *117*, 7001−7003.
(86) Harcourt, J.; Tamin, A.; Lu, X.; Kamili, S.; Sakthivel, S. K.; Murray, J.; Queen, K.; Tao, Y.; Paden, C. R.; Zhang, J.; et al. Isolation and characterization of SARS-CoV-2 from the first US COVID-19 patient. 2020, BioRxiv. https://www.biorxiv.org/content/10.1101/2020.03.02.972935v2.
(87) Okba, N. M.; Müller, M. A.; Li, W.; Wang, C.; GeurtsvanKessel, C. H.; Corman, V. M.; Lamers, M. M.; Sikkema, R. S.; de Bruin, E.; Chandler, F. D.; et al. SARS-CoV-2 specific antibody responses in COVID-19 patients. 2020, medRxiv. https://www.medrxiv.org/content/10.1101/2020.03.18.20038059v1.
(88) van Doremalen, N.; Bushmaker, T.; Morris, D. H.; Holbrook, M. G.; Gamble, A.; Williamson, B. N.; Tamin, A.; Harcourt, J. L.; Thornburg, N. J.; Gerber, S. I.; et al. Aerosol and Surface Stability of

https://doi.org/10.1021/acsomega.0c06335
ACS Omega 2021, 6, 6509−6527

SARS-CoV-2 as Compared with SARS-CoV-1. *N. Engl. J. Med.* **2020**, *382*, 1564−1567.
(89) Smither, S. J.; Lear-Rooney, C.; Biggins, J.; Pettitt, J.; Lever, M. S.; Olinger, G. G., Jr. Comparison of the plaque assay and 50% tissue culture infectious dose assay as methods for measuring filovirus infectivity. *J. Virol. Methods* **2013**, *193*, 565−571.
(90) Kraay, A. N. M.; Hayashi, M. A. L.; Hernandez-Ceron, N.; Spicknall, I. H.; Eisenberg, M. C.; Meza, R.; Eisenberg, J. N. S. Fomite-mediated transmission as a sufficient pathway: a comparative analysis across three viral pathogens. *BMC Infect. Dis.* **2018**, *18*, 540.
(91) Vega, E.; Garland, J.; Pillai, S. D. Electrostatic Forces Control Nonspecific Virus Attachmentto Lettuce. *J. Food Prot.* **2007**, *71*, 522−529.
(92) Gerba, C. P. Applied and theoretical aspects of virus adsorption to surfaces. *Adv. Appl. Microbiol.* **1984**, *30*, 133−168.
(93) Murray, J. *Physical Chemistry of Virus Adsorption and Degradation on Inorganic Surfaces: Its Relation to Wastewater Treatment*; Venosa, A. D., Ed.; Environmental Protection Technology, United States EPA: 1980.
(94) van Oss, C. J. Acid—base interfacial interactions in aqueous media. *Colloids Surf., A* **1993**, *78*, 1−49.
(95) Dang, H. T. T.; Tarabara, V. V. Virus deposition onto polyelectrolyte-coated surfaces: A study with bacteriophage MS2. *J. Colloid Interface Sci.* **2019**, *540*, 155−166.
(96) Chrysikopoulos, C. V.; Syngouna, V. I. Attachment of bacteriophages MS2 and ΦX174 onto kaolinite and montmorillonite: extended-DLVO interactions. *Colloids Surf., B* **2012**, *92*, 74−83.
(97) Attinti, R.; Wei, J.; Kniel, K.; Sims, J. T.; Jin, Y. Virus' (MS2, phiX174, and Aichi) attachment on sand measured by atomic force microscopy and their transport through sand columns. *Environ. Sci. Technol.* **2010**, *44*, 2426−2432.
(98) Dika, C.; Duval, J. F. L.; Francius, G.; Perrin, A.; Gantzer, C. Isoelectric point is an inadequate descriptor of MS2, Phi X 174 and PRD1 phages adhesion on abiotic surfaces. *J. Colloid Interface Sci.* **2015**, *446*, 327−334.
(99) Michen, B.; Graule, T. Isoelectric points of viruses. *J. Appl. Microbiol.* **2010**, *109*, 388−397.
(100) Schaldach, C. M.; Bourcier, W. L.; Shaw, H. F.; Viani, B. E.; Wilson, W. D. The influence of ionic strength on the interaction of viruses with charged surfaces under environmental conditions. *J. Colloid Interface Sci.* **2006**, *294*, 1−10.
(101) Oldham, K. B. A Gouy−Chapman−Stern model of the double layer at a (metal)/(ionic liquid) interface. *J. Electroanal. Chem.* **2008**, *613*, 131−138.
(102) Brown, M. A.; Bossa, G. V.; May, S. Emergence of a Stern Layer from the Incorporation of Hydration Interactions into the Gouy-Chapman Model of the Electrical Double Layer. *Langmuir* **2015**, *31*, 11477−11483.
(103) Armanious, A.; Aeppli, M.; Jacak, R.; Refardt, D.; Sigstam, T.; Kohn, T.; Sander, M. Viruses at Solid-Water Interfaces: A Systematic Assessment of Interactions Driving Adsorption. *Environ. Sci. Technol.* **2016**, *50*, 732−743.
(104) Chattopadhyay, S.; Puls, R. W. Forces dictating colloidal interactions between viruses and soil. *Chemosphere* **2000**, *41*, 1279−1286.
(105) Dika, C.; Ly-Chatain, M. H.; Francius, G.; Duval, J. F. L.; Gantzer, C. Non-DLVO adhesion of F-specific RNA bacteriophages to abiotic surfaces: Importance of surface roughness, hydrophobic and electrostatic interactions. *Colloids Surf., A* **2013**, *435*, 178−187.
(106) Dika, C.; Duval, J. F. L.; Ly-Chatain, H. M.; Merlin, C.; Gantzer, C. Impact of internal RNA on aggregation and electrokinetics of viruses: comparison between MS2 phage and corresponding virus-like particles. *Appl. Environ. Microbiol.* **2011**, *77*, 4939−4948.
(107) Lance, J. C.; Gerba, C. P. Effect of ionic composition of suspending solution on virus adsorption by a soil column. *Appl. Environ. Microbiol.* **1984**, *47*, 484−488.
(108) Chia, P. Y.; Coleman, K. K.; Tan, Y. K.; Ong, S. W. X.; Gum, M.; Lau, S. K.; Sutjipto, S.; Lee, P. H.; Young, B. E.; et al. Detection of Air and Surface Contamination by Severe Acute Respiratory Syndrome Coronavirus 2 (SARS-CoV-2) in Hospital Rooms of Infected Patients. 2020, medRxiv. https://www.medrxiv.org/content/10.1101/2020.03.29.20046557v2.
(109) Langlet, J.; Gaboriaud, F.; Gantzer, C.; Duval, J. F. L. Impact of chemical and structural anisotropy on the electrophoretic mobility of spherical soft multilayer particles: the case of bacteriophage MS2. *Biophys. J.* **2008**, *94*, 3293−3312.
(110) Hernando-Pérez, M.; Cartagena-Rivera, A. X.; Lošdorfer Božič, A.; Carrillo, P. J. P.; San Martín, C.; Mateu, M. G.; Raman, A.; Podgornik, R.; de Pablo, P. J. Quantitative nanoscale electrostatics of viruses. *Nanoscale* **2015**, *7*, 17289−17298.
(111) Vasickova, P.; Pavlik, I.; Verani, M.; Carducci, A. Issues Concerning Survival of Viruses on Surfaces. *Food Environ. Virol.* **2010**, *2*, 24−34.
(112) Lopez, G. U.; Gerba, C. P.; Tamimi, A. H.; Kitajima, M.; Maxwell, S. L.; Rose, J. B. Transfer efficiency of bacteria and viruses from porous and nonporous fomites to fingers under different relative humidity conditions. *Appl. Environ. Microbiol.* **2013**, *79*, 5728−5734.
(113) Julian, T. R.; Leckie, J. O.; Boehm, A. B. Virus transfer between fingerpads and fomites. *J. Appl. Microbiol.* **2010**, *109*, 1868−1874.
(114) Rusin, P.; Maxwell, S.; Gerba, C. Comparative surface-to-hand and fingertip-to-mouth transfer efficiency of gram-positive bacteria, gram-negative bacteria, and phage. *J. Appl. Microbiol.* **2002**, *93*, 585−592.
(115) Biryukov, J.; Boydston, J. A.; Dunning, R. A.; Yeager, J. J.; Wood, S.; Reese, A. L.; Ferris, A.; Miller, D.; Weaver, W.; Zeitouni, N. E.; et al. Increasing Temperature and Relative Humidity Accelerates Inactivation of SARS-CoV-2 on Surfaces. *mSphere* **2020**, *5*, 1.
(116) Chan, K. H.; Peiris, J. M.; Lam, S. Y.; Poon, L. L. M.; Yuen, K. Y.; Seto, W. H. The effects of temperature and relative humidity on the viability of the SARS coronavirus. *Adv. Virol.* **2011**, *2011*, 734690.
(117) Sobsey, M. D.; Meschke, J. S. Virus survival in the environment with special attention to survival in sewage droplets and other environmental media of fecal or respiratory origin; World Health Organization: Geneva, Switzerland, *70*, pp.19-39. 2003.
(118) Skraber, S.; Schijven, J.; Gantzer, C.; de Roda Husman, A. M. Pathogenic viruses in drinking-water biofilms: a public health risk? *Biofilms* **2005**, *2*, 105−117.
(119) Lacroix-Gueu, P.; Briandet, R.; Lévêque-Fort, S.; Bellon-Fontaine, M.-N.; Fontaine-Aupart, M.-P. In situ measurements of viral particles diffusion inside mucoid biofilms. *C. R. Biol.* **2005**, *328*, 1065−1072.
(120) Schwartz, T.; Hoffmann, S.; Obst, U. Formation of natural biofilms during chlorine dioxide and u.v. disinfection in a public drinking water distribution system. *J. Appl. Microbiol.* **2003**, *95*, 591−601.
(121) Pastorino, B.; Touret, F.; Gilles, M.; de Lamballerie, X.; Charrel, R. N. Prolonged Infectivity of SARS-CoV-2 in Fomites. *Emerging Infect. Dis.* **2020**, *26*, 2256.
(122) Firquet, S.; Beaujard, S.; Lobert, P.-E.; Sané, F.; Caloone, D.; Izard, D.; Hober, D. Survival of Enveloped and Non-Enveloped Viruses on Inanimate Surfaces. *Microbes Environ.* **2015**, *30*, 140−144.
(123) Thomas, Y.; Vogel, G.; Wunderli, W.; Suter, P.; Witschi, M.; Koch, D.; Tapparel, C.; Kaiser, L. Survival of influenza virus on banknotes. *Appl. Environ. Microbiol.* **2008**, *74*, 3002−3007.
(124) Cox, C. S. Roles of water molecules in bacteria and viruses. *Origins Life Evol. Biospheres* **1993**, *23*, 29−36.
(125) Bean, B.; Moore, B. M.; Sterner, B.; Peterson, L. R.; Gerding, D. N.; Balfour, H. H. Survival of influenza viruses on environmental surfaces. *J. Infect. Dis.* **1982**, *146*, 47−51.
(126) Page, K.; Wilson, M.; Parkin, I. P. Antimicrobial surfaces and their potential in reducing the role of the inanimate environment in the incidence of hospital-acquired infections. *J. Mater. Chem.* **2009**, *19*, 3819.
(127) Dancer, S. J. Controlling hospital-acquired infection: focus on the role of the environment and new technologies for decontamination. *Clin. Microbiol. Rev.* **2014**, *27*, 665−690.

https://doi.org/10.1021/acsomega.0c06335
ACS Omega 2021, 6, 6509−6527

(128) Walji, S.-D.; Aucoin, M. G. A critical evaluation of current protocols for self-sterilizing surfaces designed to reduce viral nosocomial infections. *Am. J. Infect. Control* **2020**, *48*, 1255.
(129) Querido, M. M.; Aguiar, L.; Neves, P.; Pereira, C. C.; Teixeira, J. P. Self-disinfecting surfaces and infection control. *Colloids Surf., B* **2019**, *178*, 8−21.
(130) Gordon, O.; Slenters, T. V.; Brunetto, P. S.; Villaruz, A. E.; Sturdevant, D. E.; Otto, M.; Landmann, R.; Fromm, K. M. Silver coordination polymers for prevention of implant infection: thiol interaction, impact on respiratory chain enzymes, and hydroxyl radical induction. *Antimicrob. Agents Chemother.* **2010**, *54*, 4208−4218.
(131) Macomber, L.; Imlay, J. A. The iron-sulfur clusters of dehydratases are primary intracellular targets of copper toxicity. *Proc. Natl. Acad. Sci. U. S. A.* **2009**, *106*, 8344−8349.
(132) Lei, H.; Jones, R. M.; Li, Y. Exploring surface cleaning strategies in hospital to prevent contact transmission of methicillin-resistant Staphylococcus aureus. *BMC Infect. Dis.* **2017**, *17*, 85.
(133) Liu, Y.; Ning, Z.; Chen, Y.; Guo, M.; Liu, Y.; Gali, N. K.; Sun, L.; Duan, Y.; Cai, J.; Westerdahl, D.; et al. Aerodynamic analysis of SARS-CoV-2 in two Wuhan hospitals. *Nature* **2020**, *582*, 557−560.
(134) Lu, J.; Gu, J.; Li, K.; Xu, C.; Su, W.; Lai, Z.; Zhou, D.; Yu, C.; Xu, B.; Yang, Z. COVID-19 Outbreak Associated with Air Conditioning in Restaurant, Guangzhou, China, 2020. *Emerging Infect. Dis.* **2020**, *26*, 1628−1631.
(135) Dietz, L.; Horve, P. F.; Coil, D. A.; Fretz, M.; Eisen, J. A.; Van Den Wymelenberg, K. 2019 Novel Coronavirus (COVID-19) Pandemic: Built Environment Considerations To Reduce Transmission. *mSystems* **2020**, *5*, No. e00245-20.
(136) Huslage, K.; Rutala, W. A.; Sickbert-Bennett, E.; Weber, D. J. A quantitative approach to defining "high-touch" surfaces in hospitals. *Infect. Control Hosp. Epidemiol.* **2010**, *31*, 850−853.
(137) Jones, R. M. Relative contributions of transmission routes for COVID-19 among healthcare personnel providing patient care. *J. Occup.. Environ. Hyg.* **2020**, *17*, 408−415.
(138) Repici, A.; Maselli, R.; Colombo, M.; Gabbiadini, R.; Spadaccini, M.; Anderloni, A.; Carrara, S.; Fugazza, A.; Di Leo, M.; Galtieri, P. A.; et al. Coronavirus (COVID-19) outbreak: what the department of endoscopy should know. *Gastrointest. Endosc.* **2020**, *92*, 192−197.
(139) Schwartz, A.; Stiegel, M.; Greeson, N.; Vogel, A.; Thomann, W.; Brown, M.; Sempowski, G. D.; Alderman, T. S.; Condreay, J. P.; Burch, J.; et al. Decontamination and Reuse of N95 Respirators with Hydrogen Peroxide Vapor to Address Worldwide Personal Protective Equipment Shortages During the SARS-CoV-2 (COVID-19) Pandemic. *Appl. Biosaf.* **2020**, *25*, 67.
(140) Koganti, S.; Alhmidi, H.; Tomas, M. E.; Cadnum, J. L.; Sass, C.; Jencson, A. L.; Donskey, C. J. Evaluation of an Ethanol-Based Spray Disinfectant for Decontamination of Cover Gowns Prior to Removal. *Infect. Control Hosp. Epidemiol.* **2017**, *38*, 364−366.
(141) Brown, T. W.; Chen, W.; Casanova, L. M. Survival and disinfection of an enveloped surrogate virus on Tyvek suits used for health care personal protective equipment. *Am. J. Infect. Control* **2016**, *44*, 1734−1735.
(142) Jinadatha, C.; Simmons, S.; Dale, C.; Ganachari-Mallappa, N.; Villamaria, F. C.; Goulding, N.; Tanner, B.; Stachowiak, J.; Stibich, M. Disinfecting personal protective equipment with pulsed xenon ultraviolet as a risk mitigation strategy for health care workers. *Am. J. Infect. Control* **2015**, *43*, 412−414.
(143) Viscusi, D. J.; Bergman, M. S.; Eimer, B. C.; Shaffer, R. E. Evaluation of five decontamination methods for filtering facepiece respirators. *Ann. Occup. Hyg.* **2009**, *53*, 815−827.
(144) Liao, L.; Xiao, W.; Zhao, M.; Yu, X.; Wang, H.; Wang, Q.; Chu, S.; Cui, Y. Can N95 Respirators Be Reused after Disinfection? How Many Times? *ACS Nano* **2020**, *14*, 6348−6356.
(145) Bessesen, M. T.; Adams, J. C.; Radonovich, L.; Anderson, J. Disinfection of reusable elastomeric respirators by health care workers: a feasibility study and development of standard operating procedures. *Am. J. Infect. Control* **2015**, *43*, 629−634.
(146) Derraik, J. G. B.; Anderson, W. A.; Connelly, E. A.; Anderson, Y. C. Rapid evidence summary on SARS-CoV-2 survivorship and disinfection, and a reusable PPE protocol using a double-hit process. 2020, medRxiv. https://www.medrxiv.org/content/10.1101/2020.04.02.20051409v1.
(147) Fischer, R. J.; Morris, D. H.; van Doremalen, N.; Sarchette, S.; Matson, M. J.; Bushmaker, T.; Yinda, C. K.; Seifert, S. N.; Gamble, A.; Williamson, B. N.; et al. Assessment of N95 respirator decontamination and re-use for SARS-CoV-2. 2020, medRxiv. https://www.medrxiv.org/content/10.1101/2020.04.11.20062018v2.
(148) Wigginton, K. R.; Pecson, B. M.; Sigstam, T.; Bosshard, F.; Kohn, T. Virus inactivation mechanisms: impact of disinfectants on virus function and structural integrity. *Environ. Sci. Technol.* **2012**, *46*, 12069−12078.
(149) Wigginton, K. R.; Kohn, T. Virus disinfection mechanisms: the role of virus composition, structure, and function. *Curr. Opin. Virol.* **2012**, *2*, 84−89.
(150) Hirose, R.; Ikegaya, H.; Naito, Y.; Watanabe, N.; Yoshida, T.; Bandou, R.; Daidoji, T.; Itoh, Y.; Nakaya, T. Survival of SARS-CoV-2 and influenza virus on the human skin: Importance of hand hygiene in COVID-19. *Clin. Infect. Dis.* **2020**, ciaa1517.
(151) van Doremalen, N.; Bushmaker, T.; Munster, V. J. Stability of Middle East respiratory syndrome coronavirus (MERS-CoV) under different environmental conditions. *Euro Surveill.* **2013**, *18*, 20590.
(152) Sizun, J.; Yu, M. W. N.; Talbot, P. J. Survival of human coronaviruses 229E and OC43 in suspension and after drying onsurfaces: a possible source ofhospital-acquired infections. *J. Hosp. Infect.* **2000**, *46*, 55−60.
(153) Warnes, S. L.; Little, Z. R.; Keevil, C. W. Human coronavirus 229E remains infectious on common touch surface materials. *MBio* **2015**, *6*, e01697−e01615.
(154) US EPA. List N: Disinfectants for Use Against SARS-CoV-2. https://www.epa.gov/pesticide-registration/list-n-disinfectants-use-against-sars-cov-2 (accessed Apr 8, 2020).
(155) Pfaender, S.; Brinkmann, J.; Todt, D.; Riebesehl, N.; Steinmann, J.; Steinmann, J.; Pietschmann, T.; Steinmann, E. Mechanisms of methods for hepatitis C virus inactivation. *Appl. Environ. Microbiol.* **2015**, *81*, 1616−1621.
(156) Lawrence, R. M.; Zook, J. D.; Hogue, B. G. Full inactivation of alphaviruses in single particle and crystallized forms. *J. Virol. Methods* **2016**, *236*, 237−244.
(157) McDonnell, G.; Russell, A. D. Antiseptics and disinfectants: activity, action, and resistance. *Clin. Microbiol. Rev.* **1999**, *12*, 147−179.
(158) ASTM. Standard Practice to Assess the Activity of Microbicides against Viruses in Suspension: Active Standard ASTM E1052. https://compass.astm.org/EDIT/html_annot.cgi?E1052+20(accessed May 10, 2020).
(159) Sattar, S. A.; Springthorpe, V. S.; Adegbunrin, O.; Zafer, A. A.; Busa, M. A disc-based quantitative carrier test method to assess the virucidal activity of chemical germicides. *J. Virol. Methods* **2003**, *112*, 3−12.
(160) Chan, K. H.; Sridhar, S.; Zhang, R. R.; Chu, H.; Fung, A. Y. F.; Chan, G.; Chan, J. F. W.; To, K. K. W.; Hung, I. F. N.; Cheng, V. C. C.; et al. Factors affecting stability and infectivity of SARS-CoV-2. *J. Hosp. Infect.* **2020**, *106*, 226−231.
(161) Rabenau, H. F.; Cinatl, J.; Morgenstern, B.; Bauer, G.; Preiser, W.; Doerr, H. W. Stability and inactivation of SARS coronavirus. *Med. Microbiol .Immunol.* **2005**, *194*, 1−6.
(162) Siddharta, A.; Pfaender, S.; Vielle, N. J.; Dijkman, R.; Friesland, M.; Becker, B.; Yang, J.; Engelmann, M.; Todt, D.; Windisch, M. P.; et al. Virucidal activity of WHO-recommended formulations against enveloped viruses including Zika, Ebola and emerging Coronaviruses. *J. Infect. Dis.* **2017**, *215*, 902.
(163) Rabenau, H. F.; Kampf, G.; Cinatl, J.; Doerr, H. W. Efficacy of various disinfectants against SARS coronavirus. *J. Hosp. Infect.* **2005**, *61*, 107−111.
(164) Eggers, M.; Eickmann, M.; Zorn, J. Rapid and Effective Virucidal Activity of Povidone-Iodine Products Against Middle East

https://doi.org/10.1021/acsomega.0c06335
ACS Omega 2021, 6, 6509−6527

Respiratory Syndrome Coronavirus (MERS-CoV) and Modified Vaccinia Virus Ankara (MVA). *Infect. Dis. Ther.* **2015**, *4*, 491−501.
(165) Ijaz, M. K.; Whitehead, K.; Srinivasan, V.; McKinney, J.; Rubino, J. R.; Ripley, M.; Jones, C.; Nims, R. W.; Charlesworth, B. Microbicidal actives with virucidal efficacy against SARS-CoV-2. *Am. J. Infect. Control* **2020**, *48*, 972−973.
(166) Sattar, S. A.; Springthorpe, V. S.; Karim, Y.; Loro, P. Chemical disinfection of non-porous inanimate surfaces experimentally contaminated with four human pathogenic viruses. *Epidemiol. Infect.* **1989**, *102*, 493−505.
(167) Goyal, S. M.; Chander, Y.; Yezli, S.; Otter, J. A. Evaluating the virucidal efficacy of hydrogen peroxide vapour. *J. Hosp. Infect.* **2014**, *86*, 255−259.
(168) Nelson, K. L.; Boehm, A. B.; Davies-Colley, R. J.; Dodd, M. C.; Kohn, T.; Linden, K. G.; Liu, Y.; Maraccini, P. A.; McNeill, K.; Mitch, W. A.; et al. Sunlight-mediated inactivation of health-relevant microorganisms in water: a review of mechanisms and modeling approaches. *Environ. Sci. Process. Impacts* **2018**, *20*, 1089−1122.
(169) Darnell, M. E. R.; Subbarao, K.; Feinstone, S. M.; Taylor, D. R. Inactivation of the coronavirus that induces severe acute respiratory syndrome, SARS-CoV. *J. Virol. Methods* **2004**, *121*, 85−91.
(170) Centers for Disease Control and Prevention. Decontamination & Reuse of N95 Respirators. https://www.cdc.gov/coronavirus/2019-ncov/hcp/ppe-strategy/decontamination-reuse-respirators.html (accessed Jul 10, 2020).
(171) Dixon, A. J.; Dixon, B. F. Ultraviolet radiation from welding and possible risk of skin and ocular malignancy. *Med. J. Aust.* **2004**, *181*, 155−157.
(172) Heilingloh, C. S.; Aufderhorst, U. W.; Schipper, L.; Dittmer, U.; Witzke, O.; Yang, D.; Zheng, X.; Sutter, K.; Trilling, M.; Alt, M.; et al. Susceptibility of SARS-CoV-2 to UV irradiation. *Am. J. Infect. Control* **2020**, *48*, 1273−1275.
(173) Simmons, S. E.; Carrion, R.; Alfson, K. J.; Staples, H. M.; Jinadatha, C.; Jarvis, W. R.; Sampathkumar, P.; Chemaly, R. F.; Khawaja, F.; Povroznik, M.; et al. Deactivation of SARS-CoV-2 with pulsed-xenon ultraviolet light: Implications for environmental COVID-19 control. *Infect. Control Hosp. Epidemiol.* **2020**, 1−130.
(174) Kanai, T.; Nakashima, S.; Oki, T. Protection against a wide UV wavelength range by Bragg reflection from polycrystalline colloidal photonic crystals. *J. Mater. Chem. C* **2019**, *7*, 7512−7515.
(175) Elhafi, G.; Naylor, C. J.; Savage, C. E.; Jones, R. C. Microwave or autoclave treatments destroy the infectivity of infectious bronchitis virus and avian pneumovirus but allow detection by reverse transcriptase-polymerase chain reaction. *Avian Pathol.* **2004**, *33*, 303−306.
(176) Michels, H. T.; Noyce, J. O.; Keevil, C. W. Effects of temperature and humidity on the efficacy of methicillin-resistant Staphylococcus aureus challenged antimicrobial materials containing silver and copper. *Lett. Appl. Microbiol.* **2009**, *49*, 191−195.
(177) Nuanualsuwan, S.; Cliver, D. O. Capsid functions of inactivated human picornaviruses and feline calicivirus. *Appl. Environ. Microbiol.* **2003**, *69*, 350−357.
(178) Eischeid, A. C.; Meyer, J. N.; Linden, K. G. UV disinfection of adenoviruses: molecular indications of DNA damage efficiency. *Appl. Environ. Microbiol.* **2009**, *75*, 23−28.
(179) Fumian, T. M.; Guimarães, F. R.; Pereira Vaz, B. J.; da Silva, M. T. T.; Muylaert, F. F.; Bofill-Mas, S.; Gironés, R.; Leite, J. P. G.; Miagostovich, M. P. Molecular detection, quantification and characterization of human polyomavirus JC from waste water in Rio De Janeiro, Brazil. *J. Water Health* **2010**, *8*, 438−445.
(180) Pecson, B. M.; Ackermann, M.; Kohn, T. Framework for using quantitative PCR as a nonculture based method to estimate virus infectivity. *Environ. Sci. Technol.* **2011**, *45*, 2257−2263.
(181) Li, J. W.; Xin, Z. T.; Wang, X. W.; Zheng, J. L.; Chao, F. H. Mechanisms of inactivation of hepatitis a virus by chlorine. *Appl. Environ. Microbiol.* **2002**, *68*, 4951−4955.
(182) Sewell, B. T.; Bouloukos, C.; Holt, C. Formaldehyde and glutaraldehyde in the fixation of chromatin for electron microscopy. *J. Microsc.* **1984**, *136*, 103−112.
(183) Gorman, S. P.; Scott, E. M.; Russell, A. D. Antimicrobial activity, uses and mechanism of action of glutaraldehyde. *J. Appl. Bacteriol.* **1980**, *48*, 161−190.
(184) Pecson, B. M.; Martin, L. V.; Kohn, T. Quantitative PCR for determining the infectivity of bacteriophage MS2 upon inactivation by heat, UV-B radiation, and singlet oxygen: advantages and limitations of an enzymatic treatment to reduce false-positive results. *Appl. Environ. Microbiol.* **2009**, *75*, 5544−5554.
(185) Warnes, S. L.; Summersgill, E. N.; Keevil, C. W. Inactivation of murine norovirus on a range of copper alloy surfaces is accompanied by loss of capsid integrity. *Appl. Environ. Microbiol.* **2015**, *81*, 1085−1091.
(186) Warnes, S. L.; Keevil, C. W. Inactivation of norovirus on dry copper alloy surfaces. *PLoS One* **2013**, *8*, No. e75017.
(187) Noyce, J. O.; Michels, H.; Keevil, C. W. Inactivation of influenza A virus on copper versus stainless steel surfaces. *Appl. Environ. Microbiol.* **2007**, *73*, 2748−2750.
(188) Schmidt, M. G.; Attaway, H. H.; Fairey, S. E.; Howard, J.; Mohr, D.; Craig, S. Self-Disinfecting Copper Beds Sustain Terminal Cleaning and Disinfection Effects throughout Patient Care. *Appl. Environ. Microbiol.* **2019**, *86*, 1.
(189) Foster, H. A.; Ditta, I. B.; Varghese, S.; Steele, A. Photocatalytic disinfection using titanium dioxide: spectrum and mechanism of antimicrobial activity. *Appl. Microbiol. Biotechnol.* **2011**, *90*, 1847−1868.
(190) Kubacka, A.; Diez, M. S.; Rojo, D.; Bargiela, R.; Ciordia, S.; Zapico, I.; Albar, J. P.; Barbas, C.; Dos Santos, V. A. M.; Fernández-García, M.; et al. Understanding the antimicrobial mechanism of TiO_2-based nanocomposite films in a pathogenic bacterium. *Sci. Rep.* **2014**, *4*, 4134.
(191) Zahid, M.; Papadopoulou, E. L.; Suarato, G.; Binas, V. D.; Kiriakidis, G.; Gounaki, I.; Moira, O.; Venieri, D.; Bayer, I. S.; Athanassiou, A. Fabrication of Visible Light-Induced Antibacterial and Self-Cleaning Cotton Fabrics Using Manganese Doped TiO_2 Nanoparticles. *ACS Appl. Bio Mater.* **2018**, *1*, 1154−1164.
(192) PureHealth. Clean Project. http://purehealth.it/ (accessed Jul 22, 2020).
(193) Weber, D. J.; Rutala, W. A. Self-disinfecting surfaces: review of current methodologies and future prospects. *Am. J. Infect. Control* **2013**, *41*, S31−S35.
(194) Hoffmann, C.; Berganza, C.; Zhang, J. Cold Atmospheric Plasma: methods of production and application in dentistry and oncology. *Med. Gas Res.* **2013**, *3*, 21.
(195) Filipić, A.; Primc, G.; Zaplotnik, R.; Mehle, N.; Gutierrez-Aguirre, I.; Ravnikar, M.; Mozetič, M.; Žel, J.; Dobnik, D. Cold atmospheric plasma as a novel method for inactivation of potato virus Y in water samples. *Food Environ. Virol.* **2019**, *11*, 220−228.
(196) Memarzadeh, F.; Olmsted, R. N.; Bartley, J. M. Applications of ultraviolet germicidal irradiation disinfection in health care facilities: effective adjunct, but not stand-alone technology. *Am. J. Infect. Control* **2010**, *38*, S13−S24.
(197) AquaPhoenix Scientific. *Sodium Hypochlorite, 13%*; AquaPhoenix Scientific: Hanover, PA, 2014.
(198) Dellanno, C.; Vega, Q.; Boesenberg, D. The antiviral action of common household disinfectants and antiseptics against murine hepatitis virus, a potential surrogate for SARS coronavirus. *Am. J. Infect. Control* **2009**, *37*, 649−652.
(199) Fisher Scientific. *Ethanol, Absolute*; Fisher Scientific: Fair Lawn, NJ. https://fscimage.fishersci.com/msds/89308.htm(accessed May 19, 2020).
(200) Spectrum Laboratory Products Inc. *Povidone-Iodine*; Spectrum Laboratory Products Inc.: Gardena, CA, 2003.
(201) Becton Dickinson Medical Systems. *EZ-SCRUB Scrub Brush 3% Chloroxylenol*; Becton Dickinson Medical Systems: Sandy, UT, 2002.
(202) First Priority, Inc. *Chlorhexidine Solution 2%*; First Priority, Inc.: Elgin, IL, 2015.
(203) Fisher Scientific. *Benzalkonium chloride 50 wt%*; Fisher Scientific: Fair Lawn, NJ, 2018.

https://doi.org/10.1021/acsomega.0c06335
ACS Omega 2021, 6, 6509−6527

(204) Reckitt Benckiser. LYSOL Brand III Disinfectant Spray; Reckitt Benckiser: Parsippany, NJ, 2012.
(205) Chen, Z.; Garcia, G., Jr.; Arumugaswami, V.; Wirz, R. E. Cold atmospheric plasma for SARS-CoV-2 inactivation. *Phys. Fluids (1994)* **2020**, *32*, 111702.
(206) Guo, J.; Huang, K.; Wang, J. Bactericidal effect of various non-thermal plasma agents and the influence of experimental conditions in microbial inactivation: A review. *Food Control* **2015**, *50*, 482−490.
(207) Hongzhuan, Z.; Ying, T.; Xia, S.; Jinsong, G.; Zhenhua, Z.; Beiyu, J.; Yanyan, C.; Lulu, L.; Jue, Z.; Bing, Y.; et al. Preparation of the inactivated Newcastle disease vaccine by plasma activated water and evaluation of its protection efficacy. *Appl. Microbiol. Biotechnol.* **2020**, *104*, 107−117.
(208) Guo, L.; Xu, R.; Gou, L.; Liu, Z.; Zhao, Y.; Liu, D.; Zhang, L.; Chen, H.; Kong, M. G. Mechanism of Virus Inactivation by Cold Atmospheric-Pressure Plasma and Plasma-Activated Water. *Appl. Environ. Microbiol.* **2018**, *84*, No. e00726-18.
(209) Sattar, S. A.; Springthorpe, V. S.; Tetro, J.; Vashon, R.; Keswick, B. Hygienic hand antiseptics: should they not have activity and label claims against viruses? *Am. J. Infect. Control* **2002**, *30*, 355−372.
(210) Kampf, G.; Kramer, A. Epidemiologic background of hand hygiene and evaluation of the most important agents for scrubs and rubs. *Clin. Microbiol. Rev.* **2004**, *17*, 863−893.
(211) CDC. Show Me the Science - How to Wash Your Hands. https://www.cdc.gov/handwashing/show-me-the-science-handwashing.html (accessed Apr 18, 2020).
(212) Luby, S. P.; Agboatwalla, M.; Billhimer, W.; Hoekstra, R. M. Field trial of a low cost method to evaluate hand cleanliness. *Trop. Med. Int. Health* **2007**, *12*, 765−771.
(213) Todd, E. C. D.; Michaels, B. S.; Smith, D.; Greig, J. D.; Bartleson, C. A. Outbreaks where food workers have been implicated in the spread of foodborne disease. Part 9. Washing and drying of hands to reduce microbial contamination. *J. Food Prot.* **2010**, *73*, 1937−1955.
(214) Jensen, D. A.; Danyluk, M. D.; Harris, L. J.; Schaffner, D. W. Quantifying the effect of hand wash duration, soap use, ground beef debris, and drying methods on the removal of Enterobacter aerogenes on hands. *J. Food Prot.* **2015**, *78*, 685−690.
(215) Fuls, J. L.; Rodgers, N. D.; Fischler, G. E.; Howard, J. M.; Patel, M.; Weidner, P. L.; Duran, M. H. Alternative hand contamination technique to compare the activities of antimicrobial and nonantimicrobial soaps under different test conditions. *Appl. Environ. Microbiol.* **2008**, *74*, 3739−3744.
(216) Boyce, J. M.; Pittet, D. Guideline for Hand Hygiene in Health-Care Settings https://www.cdc.gov/mmwr/preview/mmwrhtml/rr5116a1.htm (accessed Apr 21, 2020).
(217) Rotter, M.; Sattar, S.; Dharan, S.; Allegranzi, B.; Mathai, E.; Pittet, D. Methods to evaluate the microbicidal activities of hand-rub and hand-wash agents. *J. Hosp. Infect.* **2009**, *73*, 191−199.
(218) Mbithi, J. N.; Springthorpe, V. S.; Sattar, S. A. Comparative in vivo efficiencies of hand-washing agents against hepatitis A virus (HM-175) and poliovirus type 1 (Sabin). *Appl. Environ. Microbiol.* **1993**, *59*, 3463−3469.
(219) Steinmann, J. Some principles of virucidal testing. *J. Hosp. Infect.* **2001**, *48*, S15−S17.
(220) ASTM. *Determining the Virus-Eliminating Effectiveness of Hygienic Handwash and Handrub Agents Using the Fingerpads of Adults*; E1838; Standard 17; ASTM International, 2017.
(221) WHO. *WHO Guidelines on Hand Hygiene in Health Care*; Patient Safety; World Health Organization, 2009.
(222) Francolini, I.; Vuotto, C.; Piozzi, A.; Donelli, G. Antifouling and antimicrobial biomaterials: an overview. *APMIS* **2017**, *125*, 392−417.

NOTE ADDED AFTER ISSUE PUBLICATION

This article was initially published with an incorrect copyright statement and was corrected on or around May 5, 2021.

https://doi.org/10.1021/acsomega.0c06335
ACS Omega 2021, 6, 6509−6527